Available online at www.sciencedirect.com
ScienceDirect
Journal of Computational Physics 226 (2007) 897–924
JOURNAL OF COMPUTATIONAL PHYSICS
www.elsevier.com/locate/jcp

Comparative analysis of multiscale Gaussian random field simulation algorithms

Peter R. Kramer [a,*], Orazgeldi Kurbanmuradov [b], Karl Sabelfeld [c,d]

[a] Department of Mathematical Sciences, Rensselaer Polytechnic Institute, Troy, NY 12180, USA
[b] Center for Phys. Math. Research, Turkmenian State University, Saparmyrat Turkmenbashy av. 31, 744000 Ashgabad, Turkmenistan
[c] Weierstrass Institute for Applied Analysis and Stochastics, Mohrenstraße 39, D-10117 Berlin, Germany
[d] Institute of Computational Mathematics and Mathematical Geophysics, Russian Acad. Sci., Lavrentieva str., 6, 630090 Novosibirsk, Russia

Received 21 December 2005; received in revised form 16 April 2007; accepted 3 May 2007
Available online 22 May 2007

Abstract

We analyze and compare the efficiency and accuracy of two simulation methods for homogeneous random fields with multiscale resolution. We consider in particular the Fourier-wavelet method and three variants of the Randomization method: (A) without any stratified sampling of wavenumber space, (B) with stratified sampling of wavenumbers with equal energy subdivision, (C) with stratified sampling with a logarithmically uniform subdivision. We focus primarily on fractal Gaussian random fields with Kolmogorov-type spectra. Previous work has shown that variants (A) and (B) of the Randomization method are only able to generate a self-similar structure function over three to four decades with reasonable computational effort. By contrast, variant (C), along with the Fourier-wavelet method, is able to reproduce accurate self-similar scaling of the structure function over a number of decades increasing linearly with computational effort (for our examples we will show that nine decades can be reproduced). We provide some conceptual and numerical comparison of the various cost contributions to each random field simulation method.

We find that when evaluating ensemble-averaged quantities like the correlation and structure functions, as well as some multi-point statistical characteristics, the Randomization method can provide good accuracy with less cost than the Fourier-wavelet method. The cost of the Randomization method relative to the Fourier-wavelet method, however, appears to increase with the complexity of the random field statistics which are to be calculated accurately. Moreover, the Fourier-wavelet method has better ergodic properties, and hence becomes more efficient for the computation of spatial (rather than ensemble) averages which may be important in simulating the solutions to partial differential equations with random field coefficients.

MSC: 60H35; 65C05

Keywords: Monte Carlo; Random field simulation; Randomization; Fourier wavelet; Multiscale

* Corresponding author. Tel.: +1 518 276 6896; fax: +1 518 276 4824.
E-mail addresses: kramep@rpi.edu (P.R. Kramer), kurbanmuradov@yandex.ru (O. Kurbanmuradov), sabelfel@wias-berlin.de (K. Sabelfeld).
URL: http://www.rpi.edu/~kramep (P.R. Kramer).

0021-9991/$ - see front matter
doi:10.1016/j.jcp.2007.05.002

1. Introduction

Random functions (generally referred to as random fields) provide a useful mathematical framework for representing disordered heterogeneous media in theoretical and computational studies. One example is in turbulent transport [10,11,16,20,26,29,41,44,45], where the velocity field representing the turbulent flow is modeled as a random field $\vec{v}(\vec{x},t)$ with statistics encoding important empirical features, and the temporal dynamics of the position $\vec{X}(t)$ and velocity $\vec{V}(t)=\frac{d\vec{X}}{dt}$ of immersed particles is then governed by equations involving this random field such as

$$m\,d\vec{V}(t) = -\gamma(\vec{V}(t)-\vec{v}(\vec{X}(t),t))\,dt + \sqrt{2k_B T\gamma}\,d\vec{W}(t), \tag{1}$$

where m is particle mass, γ is its friction coefficient, k_B is Boltzmann's constant, T is the absolute temperature, and $\vec{W}(t)$ is a random Wiener process representing molecular collisions. Another example is in transport through porous media, such as groundwater aquifers, in which the hydraulic conductivity $\mathsf{K}(\vec{x})$ is modeled as random field reflecting the empirical variability of the porous medium [39,18,5,22]. The Darcy flow rate $\vec{q}(\vec{x})$ in response to pressure applied at the boundary is governed by the Darcy equation

$$\begin{aligned} &\vec{q}(\vec{x}) = -\mathsf{K}(\vec{x})\,\mathrm{grad}\,\phi(\vec{x}),\\ &\mathrm{div}\,\vec{q} = 0, \end{aligned} \tag{2}$$

in which the random hydraulic conductivity function appears as a coefficient, and the applied pressure is represented in the boundary conditions for the internal pressure head ϕ. Our concern is with the computational simulation of random fields for applications such as these.

Interesting insights into the dynamics of transport in disordered media can be achieved already through relatively simple random models for the velocity field, such a finite superposition of Fourier modes, with each amplitude independently evolving according to an Ornstein–Uhlenbeck process [3,44]. Here efficient and accurate numerical simulations of the flow can be achieved through application of the well-developed literature on simulating stochastic ordinary differential equations [21]. We will focus instead on the question of simulating random fields which involve challenging multiscale structures such as those relevant to porous media and turbulent flow simulations. Many questions remain open for the case of Gaussian multiscale random fields, so we confine our attention to this class.

We shall give a general description of homogeneous random field representations in multi-dimensional Euclidean space $\mathbb{R}^d$ in the introductory Sections 1 and 2. In the main part of the paper (Sections 3–8) we deal with the context of real-valued scalar random fields on the real line.

Under quite general conditions, a real-valued Gaussian homogenous random field $u(\vec{x})$ can be represented through a stochastic Fourier integral [34]

$$u(\vec{x}) = \int_{\mathbb{R}^d} e^{-2\pi i\vec{k}\cdot\vec{x}} E^{1/2}(\vec{k})\tilde{W}(d\vec{k}), \tag{3}$$

where $\tilde{W}(d\vec{k})$ is a complex-valued white noise random measure on $\mathbb{R}^d$, with $\tilde{W}(B)=\overline{\tilde{W}(-B)}$, $\langle\tilde{W}(B)\rangle=0$, and $\langle\tilde{W}(B)\overline{\tilde{W}(B')}\rangle=\mu(B\cap B')$ for Lebesgue measure μ and all Lebesgue-measurable sets B, B'. We use angle brackets $\langle\cdot\rangle$ to denote statistical (ensemble) averages. The spectral density $E(\vec{k})$ is a nonnegative even function representing the strength (energy) of the random field associated to the wavenumber $\vec{k}$, meaning the length scale $1/|\vec{k}|$ and direction $\vec{k}/|\vec{k}|$.

Multiscale random fields will have a multiscale spectral density, meaning that $E(\vec{k})$ will have substantial contributions over a wide range of wavenumbers $k_{\min}\ll|\vec{k}|\ll k_{\max}$, with $k_{\max}/k_{\min}\gg 1$. This poses a challenge for efficient simulation.

Several approaches are based on various discretizations of (3) which give rise to finite sums of functions with independent Gaussian random coefficients [38]. A Riemann sum discretization of the stochastic integral is easy to implement [15,35,43,46,47], and following [7,19,29], we shall refer to it as the standard Fourier method. As documented in [7], this method can suffer from false periodicity artifacts of the discretization, particularly if the wavenumbers are chosen with uniform spacing.

An alternative "Randomization method" has been developed which evaluates the stochastic integral (3) through a finite set of randomly chosen wavenumbers generated by Monte Carlo methods [23,33]. Yet another method designed for multiscale random field simulation is the Fourier-wavelet method [6], which arises from a wavelet decomposition of the white noise measure in (3). We stress that neither of these methods require that the multiscale structure be self-similar, though they are well-suited for this special case. The Fourier-wavelet and Randomization methods have been previously studied and compared, particularly in the context of (massless) turbulent diffusion problems [2,6], with the general conclusion that the Randomization method performs well for simulating random fields with a self-similar multiscale scaling structure extending over a small number of decades, while the Fourier-wavelet method becomes more efficient for random fields with a large number of decades of self-similar scaling. The methods also have some theoretical differences. The Randomization method reproduces the correlation function (or structure function) with only sampling error and no bias, while the Fourier-wavelet method incurs some bias from the truncation of the sums in the associated random field representations, which can however be significantly reduced through a good choice of wavelet functions [8,6]. On the other hand, the Fourier-wavelet method simulates a truly Gaussian random field, while the statistics of quantities involving two or more evaluation points are generally simulated as non-Gaussian by the Randomization method. However, as more wavenumbers are included in the random field representation, central limit theorem arguments indicate that the statistics simulated by the Randomization method should approach Gaussian values [24]. In particular, the simulations of fractal random fields in [6] indicate that the kurtosis (normalized fourth order moment) of spatial increments in the random field was close to its Gaussian value of 3 over a range of scales which was one or two decades fewer than the range over which the second order moments were accurately simulated.

In the comparisons [2,6], a particular version of the Randomization method was used; namely, the random wavenumbers were chosen according to a stratified sampling strategy with a subdivision of wavenumber space into sampling bins of equal energy. In the studies [40,26], a logarithmically stratified subdivision of wavenumber space was found to be significantly more efficient in representing self-similar power-law spectra such as those corresponding to Kolmogorov turbulence. This implementation of the Randomization method [26], a similar implementation of the standard Fourier method with wavenumber discretized uniformly and deterministically in logarithmic space [45], and a multiscale wavelet method [10] have all been employed to simulate dispersion of pair particles in isotropic Gaussian frozen pseudoturbulence with a Kolmogorov spectrum extending over several decades, in some cases with a constant mean sweep. Of particular interest in these works is whether the classical Richardson's cubic law can be observed in numerically generated pseudoturbulence [26,45,10].

We investigate the efficiency and accuracy of the Fourier-wavelet and Randomization methods, including alternative strategies for stratified sampling, along the following directions:

- The previous studies of which we are aware [2,6] focus on the cost of simulating the value of the random field at a particular point x on demand, as is appropriate in the turbulent diffusion problem (1). By contrast, the solution of the porous medium problem requires the generation of the random field over the whole computational domain at once. We consider how the computational cost of the Randomization and Fourier-wavelet methods compare for various tasks in which the random field is to be evaluated at a set of points specified in advance or on demand, regularly or irregularly distributed within the computational domain. Both the overhead cost and the cost of simulating each new realization of the random field is considered.
- We study statistical features of the random field beyond two-point quantities such as the second order structure function

$$D(\rho) = \langle (u(x+\rho) - u(x))^2 \rangle \tag{4}$$

and associated kurtosis which have been the focus of previous work [6,2]. We point out that the Randomization method has the flexibility to simulate a random field using a smaller set of random variables than the Fourier-wavelet method, which permits for example the faster simulation of a random field with good accuracy of the simulated second order structure function. We examine how the number of random variables (and associated simulation cost) required by the Randomization method changes when more complex multi-point statistics are to be simulated accurately.

- We study the ergodicity properties of the simulation methods, which we expect to be important in the accurate simulation of statistics of the solutions of partial differential equations with random field coefficients such as the Darcy equation (2).

We begin in Section 2 by identifying some physical and numerical parameters which will play a key role in the development of the simulation algorithms and in quantifying their costs. We then present a brief but self-contained description of the Randomization method (Section 3) and the Fourier-wavelet method (Section 4), framing the discussion primarily in terms of one-dimensional random functions for notational simplicity. We begin our examination of the numerical methods with a theoretical discussion in Section 5 of how their costs should scale with respect to various physical and numerical implementation parameters. We then revisit the question studied in [2,6] concerning the comparative ability of the methods to generate random fields with self-similar fractal scaling of the second order structure functions over a large number of decades. Our contribution here is to consider variations of the Randomization method which significantly improve its performance. We then turn to comparisons of the ergodic properties (Section 6) and the quality of the multi-point statistics of the random fields (Section 7) simulated by the Randomization method and Fourier-wavelet method. Our findings are summarized in Section 8.

The general conclusions are that the use of a logarithmically uniform stratified sampling strategy for the Randomization method greatly increases its competitiveness with the Fourier-wavelet method for simulating multiscale random fields. The Randomization method can simulate low order statistics such as the second order structure function (4) and associated kurtosis accurately using a smaller number of random variables and therefore lower cost than the Fourier-wavelet method. The cost of the Randomization method relative to the Fourier-wavelet method, however, increases with the number of observation points involved in the statistic to be simulated. In particular, to have good ergodic properties, meaning the accurate simulation of the statistics of spatial averages over large regions, the Randomization method incurs a cost considerably larger than the Fourier-wavelet method. The choice of which method to be used in the simulation of a multiscale random field in an application, therefore, should be guided by what types of statistics of the random field need to be simulated accurately. The Randomization method is simpler to implement and is faster for the accurate simulation of statistics involving a relatively small number of observation points. The Fourier-wavelet method is somewhat more complicated, but appears to be considerably more efficient in the accurate simulation of statistics involving large numbers of points, particularly ergodic averages.

2. General simulation framework

To discuss the implementation and the costs of the simulation methods, we first delimit the questions to be asked about the random field $u(\vec{x})$ to be simulated. We suppose here that $u(\vec{x})$ is a well-defined scalar-valued homogenous, Gaussian random field with given spectral density $E(\vec{k})$ which is just the Fourier transform of the correlation function $\mathsf{B}(\vec{r}) = \langle u(\vec{x}+\vec{r})u(\vec{x})\rangle$:

$$\mathsf{B}(r) = \int_{\mathbb{R}^d} \exp\{2\pi \mathrm{i}\vec{k}\cdot\vec{r}\}E(\vec{k})\,\mathrm{d}\vec{k}, \quad E(\vec{k}) = \int_{\mathbb{R}^d} \exp\{-2\pi\mathrm{i}\vec{k}\cdot\vec{r}\}\mathsf{B}(\vec{r})\,\mathrm{d}\vec{r}.$$

The simulation of vector-valued multiscale Gaussian random fields can be conducted through standard extensions from the scalar-valued case. We quantify first in Section 2.1 some fundamental length scales of the random field which play a key role in choosing simulation parameters, then discuss in Section 2.2 some further length scales determined by the context of the problem or the choice of numerical implementation.

2.1. Length scales of the random field

One of the most fundamental quantitative properties of a random field is its *correlation length*, which we define as:

$$\ell_c = \left(V_d^{-1} \frac{\sup_{\vec{k}\in\mathbb{R}^d} E(\vec{k})}{\int_{\mathbb{R}^d} E(\vec{k})\,\mathrm{d}\vec{k}} \right)^{1/d}, \tag{5}$$

where $V_d = 2\pi^{d/2}/(d\Gamma(d/2))$ is the volume of the unit ball in d dimensions ($V_1 = 2,\ V_2 = \pi,\ V_3 = 4\pi/3$). The usual definition [32] has simply $E(\vec{0})$ in the numerator, but our definition generalizes meaningfully to random fields with the spectral density vanishing at the origin. Indeed $E(\vec{0})$ is the integral of the trace of the correlation function, which under many conditions gives the product of the random field variance and the correlation volume. The denominator precisely cancels out the random field variance $\langle u^2 \rangle$, and the remaining operations convert the correlation volume to a correlation length. If however the random field has oscillations, the integral of the correlation function may underrepresent the actual correlation volume (including the extent of negative correlations). This is why we have simply modified the definition to involve the value of the spectral density at its peak wavenumber; it coincides of course with the standard convention in the case of random fields with spectral density peaked at the origin (as is often the case in the absence of strong negative correlations in the random field).

We similarly define a *smoothness microscale* for the random field:

$$\ell_s = \left(V_d^{-1} \frac{\sup_{\vec{k} \in \mathbb{R}^d} |\vec{k}|^2 E(\vec{k})}{\int_{\mathbb{R}^d} |\vec{k}|^2 E(\vec{k})\, \mathrm{d}\vec{k}} \right)^{1/d}, \tag{6}$$

which is really an analogous correlation length for the random field gradient $\vec{\nabla} u$. The two length scales ℓ_c and ℓ_s generalize the notion of integral length scale and Kolmogorov dissipation length scale in turbulent spectra to general homogenous random fields. The correlation length can be thought of as the largest length scale on which the random field $u(\vec{x})$ exhibits a nontrivial correlation structure. That is, for $|\vec{x} - \vec{x}'| \gg \ell_c$, the values of $u(\vec{x})$ and $u(\vec{x}')$ are independent to a good approximation. The smoothness microscale, conversely, describes the smallest length scale on which the random field has nontrivial correlation structure. On smaller scales, the random field appears smooth. More precisely, for $|\vec{x} - \vec{x}'| \ll \ell_s$, the random field over the line segment connecting $\vec{x}$ and $\vec{x}'$ can be well approximated by a linear interpolation between $u(\vec{x})$ and $u(\vec{x}')$ (with *relative* error $o(|\vec{x} - \vec{x}'|/\ell_s)$).

We will contemplate only random fields with spectral density behaving well enough at small and large wavenumbers to be integrable, so that the correlation length ℓ_c in (5) is well-defined as a finite nonzero value. We admit random fields for which the integral in the denominator of (6) converges or diverges; in the latter case, we define $\ell_s = 0$. Idealized fractal random fields [31,12], such as those associated with the Kolmogorov inertial range theory of turbulence $E(\vec{k}) \propto |\vec{k}|^{-5/3}$ can be placed within the present framework if we agree from the outset that the fractal scaling is smoothed out at a pre-defined large length scale. This will be appropriate for any physical application, and even from a purely mathematical point of view, we can think of this length scale cutoff as defining a concrete goal for the simulation of a fractal random field with finite effort. Any numerical simulation or physical application will also necessarily have a positive lower limit on the length scale of fractal scaling, but we do not need to enforce this within our mathematical framework.

For some random fields, the smoothness length scale is comparable to the correlation length. This is true in particular if the random field depends only on one physical length scale. For such "single-scale" Gaussian homogenous random fields, a wide variety of simulation techniques beyond the Fourier-wavelet and Randomization methods may well be adequate [35]. Our concern is with simulating multiscale random fields, meaning that $\ell_s \ll \ell_c$. One situation where this can arise is in two-scale random fields (such as those contemplated in homogenization theory [4]), where $E(\vec{k})$ is peaked near widely separated wavenumbers $|\vec{k}| \sim \ell_c^{-1}$ and $|\vec{k}| \sim \ell_s^{-1}$ but rapidly decaying away from these values. In this case, the random field could be simulated simply by expressing it as the superposition of two independent single-scale random fields, one varying on the large scale, and one on the small scale. But in applications such as turbulence and porous media flow, and in any context involving fractal random models, the spectral density has nontrivial contributions over a great range of wavenumbers within the wide interval $\ell_c^{-1} \ll |\vec{k}| \ll \ell_s^{-1}$, and the random field is not well-approximated by a superposition of a few single-scale random fields. These are the situations in which the power of the Fourier-wavelet and Randomization methods is indicated, and that we will focus on in most of this paper. In particular, we consider power-law spectra extending from a wavenumber ℓ_c^{-1} to ℓ_s^{-1} with $\ell_s \ll \ell_c$ (including the case $\ell_s = 0$) as multiscale fields. Even though such an energy spectrum can be defined with one or two length scales, it cannot be simulated efficiently by a superposition of single-scale methods because the random field has

substantial energy on all the length scales between the widely separated lengths ℓ_s and ℓ_c, in contrast to the two-scale fields amenable to homogenization theory discussed earlier in the paragraph.

2.2. Length scales introduced in computation

In some applications, we may need to evaluate the random field at a pre-specified set of points in d dimensions. One example would be the simulation of the flow through a porous medium [18,39], in which the random field would need to be simulated on a computational grid over an entire pre-defined region. For this to require finite computational work, we must agree upon a domain length scale L and a sampling length scale h. The domain length scale describes the linear extent of the region over which the random field is evaluated, and the sampling length denotes the distance between points at which the random field is calculated. In the simplest case, the random field is to be simulated on a Cartesian grid with linear extent L in each direction, with grid spacing h. We can however consider the more general situation in which the prespecified points are irregularly arranged. Our computational cost considerations will still apply provided that the collection of points can still be described meaningfully by a characteristic length scale L of the overall diameter of the cluster of points and a length scale h for the typical separation between neighboring points.

In other applications, such as the simulation of a particle moving through a prescribed turbulent field (1), one may wish to be able to evaluate the random field $u(\vec{x})$ at arbitrary points on demand (not known in advance of the generation of the random field). In situations in which the points to be specified on demand are expected to be rather densely distributed over a fixed computational domain, one might approach this simulation task by laying down a grid of points over the domain, pre-computing the random field over this grid, and then interpolating from this computed grid of random field values to evaluate the random field at points which are requested later. Since the interpolation procedure is separate from the type of algorithm used to simulate the multiscale Gaussian random field, it will not concern us. The cost and considerations involved in simulating the random field on the grid for interpolation falls within the category of random field simulations over a pre-specified set of points. On the other hand, if the points at which the random field is to be evaluated are not known to fall within a particular computational domain or if the evaluation points are expected to be rather sparsely distributed in the computational domain, then the strategy of pre-computation of the random field over a grid followed by interpolation may be impractical or inefficient. In this case, the computational procedure truly involves the evaluation of the simulated random field representation at an arbitrary collection of points not known in advance. This task has been the emphasis of previous studies of multiscale Gaussian random field simulation algorithms [42,9].

Finally, for any application, the ideal random field to be simulated has nontrivial structure on length scales ranging from ℓ_s to ℓ_c. A numerical multiscale representation of this random field will be associated with certain finite minimum and maximum length scales $\ell_{\min}$ and $\ell_{\max}$, outside of which the method cannot be expected to accurately represent the structure of the ideal random field. The length scales $\ell_{\max}$ and $\ell_{\min}$ can be related to more fundamental parameters of the Monte Carlo simulation methods, as we describe in subsequent sections. Generally speaking, $\ell_{\max}$ should be chosen to be at least as large as the correlation length ℓ_c (but need not be as large as the domain length L). On the other hand, $\ell_{\min}$ is set either equal to or somewhat smaller than $\max(h, \ell_s)$ or at a larger value determined by computational cost constraints.

3. Randomization methods

To maintain focus on the central issues of concern, we will develop the algorithms and their analysis for the case of a real-valued homogenous Gaussian scalar random field $u(x)$ defined on the one-dimensional real line. Generalizations of the algorithms to multiple dimensions can be found in [42,9], and we will occasionally comment how our theoretical discussion generalizes easily to the multi-dimensional case.

The simplest form of the Randomization method, which we shall refer to as *variant A*, reads [33,42]

$$u^{(\mathrm{R})}(x) = \frac{\sigma}{\sqrt{n_0}} \sum_{j=1}^{n_0} [\xi_j \cos(2\pi k_j x) + \eta_j \sin(2\pi k_j x)], \tag{7}$$

where ξ_j, η_j, $j = 1, \ldots, n_0$ are mutually independent standard Gaussian random variables (mean zero and unit variance), and $\sigma^2 = \int E(k)\,\mathrm{d}k = 2\int_0^\infty E(k)\,\mathrm{d}k$. The wave numbers k_j, $j = 1, \ldots, n_0$, are chosen as independent random variables in $[0, \infty)$ according to the probability density function (pdf) $p(k) = 2E(k)/\sigma^2$, and are also independent of the ξ_j and η_j. This variant A of the Randomization method may be thought of as the most straightforward way to approximate the Fourier stochastic integral (3) through a Monte Carlo integration approach, using the complex conjugacy between the simulated random variables associated to wavenumbers $\pm k$.

While the Randomization method always produces random field approximations with the correct mean and correlation function *when averaged over a theoretically complete ensemble of realizations*, the practical concern is how well one or a finite number of samples of the simulated random field replicate the statistics of the true random field which is to be simulated. The randomization of the choice of wavenumbers creates some additional variability in the simulated random field (such as realizations where, say, the low wavenumbers happen to be undersampled). A common practice in improving Monte Carlo calculations is the employment of "variance reduction" techniques which constrain the random choices somewhat to mitigate the problem of generating an artificially large number of strongly deviant samples. An extreme remedy would be to prescribe the wavenumbers deterministically, as in the standard Fourier method discussed in Section 1, but this has its own artifacts [7].

A compromise which seeks to avoid the problems of both purely deterministic and purely random choices of random wavenumbers is to partition wavenumber space into bins, and to choose a prescribed number of wavenumbers at random locations within each bin. This Monte Carlo variance reduction technique is an example of "stratified sampling" [37,42]. It ensures a certain coverage of wavenumber space, but still takes advantage of Monte Carlo integration techniques.

The mathematical framework for stratified sampling in the Randomization method is given as follows. We take Δ as the total space from which the wavenumbers are to be sampled (it can in general be chosen as $\Delta = [0, \infty)$ but it can also be chosen as the possibly smaller support of the spectrum E on the nonnegative real axis. We then choose a partition of Δ into a union of smaller non-overlapping intervals $\Delta = \bigcup_{j=1}^n \Delta_j$. Within each interval Δ_j, we sample n_0 independent random wavenumbers k_{jl}, $l = 1, \ldots, n_0$, according to the probability distribution function

$$p_j(k) \equiv \begin{cases} \frac{2E(k)}{\sigma_j^2} & \text{for } k \in \Delta_j, \\ 0 & \text{for } k \notin \Delta_j, \end{cases}$$

where

$$\sigma_j^2 = 2\int_{\Delta_j} E(k)\,\mathrm{d}k.$$

The simulation formula then reads

$$u^{(\mathrm{R,s})}(x) = \sum_{j=1}^{n} \frac{\sigma_j}{\sqrt{n_0}} \sum_{l=1}^{n_0} [\xi_{jl}\cos(2\pi k_{jl}x) + \eta_{jl}\sin(2\pi k_{jl}x)]. \tag{8}$$

The amplitudes ξ_{jl}, η_{jl}, $j = 1, \ldots, n$; $l = 1, \ldots, n_0$, are again standard Gaussian random variables which are mutually independent and independent of the choice of wavenumbers k_{jl}. One natural choice of stratified sampling for variance reduction is to choose a number of sampling bins n and then choose the sampling intervals Δ_j so that each of them contains an equal amount of "energy" (integral of the spectral density): $\sigma_j^2 = \sigma^2/n$ for $1 \leqslant j \leqslant n$. We refer to this stratified sampling strategy as *variant B* of the Randomization method.

We will also explore an alternative stratified sampling strategy in which the sampling bins are simply assigned to be equally spaced with respect to $\ln k$. That is, the wave number intervals $\Delta_j = (\hat{k}_j, \hat{k}_{j+1}]$ for $j = 1, \ldots, n$ are defined according to a geometric distribution with ratio parameter q: $\hat{k}_{j+1} = q\hat{k}_j$, $j = 2, \ldots, n-1$. If the spectral density of the random field is confined to a bounded domain of wavenumbers $k \leqslant k_{\max}$, then we can choose $\hat{k}_{n+1} = k_{\max}$; otherwise we take $\hat{k}_{n+1} = \infty$. Similarly, if the minimal wavenumber $k_{\min}$ in the support of the spectral density is positive, we can choose $\hat{k}_1 = k_{\min}$. Otherwise, we would choose $\hat{k}_1$ in some other way suggested by the spectrum, perhaps as the wavenumber at which the

spectral density is maximal, and then adjoin a sampling bin $\Delta_0 = (0, \hat{k}_1)$. We call this stratified sampling strategy based on a logarithmically uniform subdivision *variant C* of the Randomization method.

The motivation for this externally imposed subdivision scheme is that a multiscale random field, particularly one with a self-similar fractal property, might be well represented in a hierarchical manner with a certain number of computational elements at each important "length scale", with geometrically distributed length scales. Indeed, this is precisely what the Fourier-wavelet simulation method (in fact any wavelet method) does, and appears to be one of the essential elements behind its demonstrated efficiency in simulating random fields with multiscale structure over many decades [6,9,8]. We are led to consider, therefore, how incorporating a similar distribution of wavenumbers within the Randomization approach would compare with the Fourier-wavelet method. Other externally imposed subdivision strategies may be chosen based on the spectral density of the random field to be simulated as well as the type of statistics which are sought in the application.

All variants of the Randomization method provide unbiased estimators of the correlation function of the simulated random field, meaning that these statistics can in principle be recovered with arbitrary precision through a sufficiently large sample size (though with the usual relatively slow convergence of Monte Carlo sampling), even with fixed finite values of the discretization parameters. In particular, there need not be a rigid maximal and minimal length scale, $\ell_{\max}$ and $\ell_{\min}$ within which the Randomization method confines its effort, because the wavenumber sampling bins can extend to $k = 0$ or $k = \infty$. However, in practice, the finite number n_0 of wavenumbers sampled in these bins does impose effective maximum and minimum length scales over which the random field structure can be expected to be adequately represented. We discuss this in the context of a particular example in Section 5.1.2. The quality of higher order and multi-point statistics simulated by the Randomization method is less clear; in particular the randomization of the wavenumbers makes the simulated field non-Gaussian. Central limit theorem concepts [1,25,24], however, indicate that with a sufficiently rich sampling of wavenumbers, the simulated field should have some approximately Gaussian properties. We investigate these questions in some detail in Sections 5–7.

4. Fourier-wavelet simulation method

We present here the one-dimensional formulation of the Fourier-wavelet method. A homogeneous Gaussian random field $u(x)$ can be represented using the Fourier-wavelet representation [6]:

$$u(x) = u_0 \sum_{m=-\infty}^{\infty} \sum_{j=-\infty}^{\infty} \gamma_{mj} f_m(2^m(x/\ell) - j), \tag{9}$$

where u_0 is a dimensional constant having the same dimensions as the field variable u, ℓ is an arbitrary length scale, γ_{mj} is a family of mutually independent standard Gaussian random variables, and

$$f_m(\xi) = \int_{-\infty}^{\infty} \mathrm{e}^{-2\pi \mathrm{i} \tilde{k} \xi} 2^{m/2} \tilde{E}^{1/2}(2^m \tilde{k}) \hat{\phi}(\tilde{k}) \, \mathrm{d}\tilde{k}, \tag{10}$$

where $\tilde{E}(\tilde{k})$ is a dimensionless spectral density defined through

$$\tilde{E}(\tilde{k}) = \frac{1}{\ell u_0^2} E(\tilde{k}/\ell).$$

Here, in order to ensure an efficient wavelet representation of the random field, $\hat{\phi}(k)$ is chosen as a compactly supported function which is the Fourier transform of the Meyer mother wavelet function based on a pth order perfect B-spline [6]:

$$\hat{\phi}(k) = -\mathrm{i}\,\mathrm{sign}(k)\mathrm{e}^{\mathrm{i}\pi k} b(|k|), \tag{11}$$

where

$$b(k) = \begin{cases} \sin\left(\frac{\pi}{2} v_p(3k-1)\right), & k \in \left(\frac{1}{3}, \frac{2}{3}\right], \\ \cos\left(\frac{\pi}{2} v_p\left(\frac{3}{2}k - 1\right)\right), & k \in \left(\frac{2}{3}, \frac{4}{3}\right], \\ 0, & \text{else.} \end{cases} \tag{12}$$

and the function $v_p(x)$ is defined by

$$v_p(x) = \frac{4^{p-1}}{p}\left\{[x-x_0]_+^p + [x-x_p]_+^p + 2\sum_{j=1}^{p-1}(-1)^j[x-x_j]_+^p\right\}, \tag{13}$$

where $x_j = (1/2)[\cos(((p-j)/p)\pi)+1]$, and $[a]_+ = \max(a,0)$. The positive integer parameter p is chosen in [6] equal to 2.

The representation (9) expresses the random field $u(x)$ as a hierarchical random superposition of real, deterministic functions f_m and their translates. The function f_m can be thought of as encoding the structure of $u(x)$ on the length scale $2^{-m}\ell$. This can best be seen by the dual relation between spatial lengths and Fourier wavenumbers, since f_m is completely determined by the contributions of the spectrum $E(k)$ over the interval $\frac{1}{3\ell}2^m \leqslant k \leqslant \frac{4}{3\ell}2^m$.

The implementation of the Fourier-wavelet method of course requires that the sums over m and j in (9) be truncated to finite sums. This is done through consideration of the length scales over which the random field is to be sampled.

First, we choose $\ell = \ell_{\max}$ as some convenient length scale that represents the largest length scale of the random field which we wish to resolve in our simulation. If the random field is to be simulated over a grid with spacing h, it will be convenient to choose ℓ so that $\ell/h = 2^m$ for some nonnegative integer m . By setting $\ell = \ell_{\max}$, it is now convenient to truncate the sum over m to run over $0 \leqslant m \leqslant M-1$, thereby formally representing the random field down to length scale $\ell_{\min} = 2^{1-M}\ell_{\max}$. Note that this truncated Fourier-wavelet random field representation will only incorporate information from the energy spectrum $E(k)$ over the wavenumber range $\frac{1}{3}\ell_{\max}^{-1} \leqslant k \leqslant \frac{4}{3}\ell_{\min}^{-1}$, so one should be careful that the energy outside this range can be safely neglected for the application.

We turn now to the truncation of the sum over the translation index j. It is shown in [6], that if the spectrum $E(k)$ is smooth enough then the functions $f_m(\xi)$ decay like $|\xi|^{-p}$ where p is the order of the spline used to construct the Meyer wavelet. So long as $p \geqslant 2$, then, we can choose an integer "bandwidth" cutoff b so that the total mean-square contribution from terms with $|j - 2^m x/\ell| > b$ to the random field value at x is as small as desired. When evaluating the random field $u(x)$ at a desired point x, then, only the $2b$ terms satisfying $|2^m(x/\ell) - j| \leqslant b$ are incorporated.

Hence the finitely truncated Fourier-wavelet representation for the value of the random field at any location x can be written as follows

$$u^{(\mathrm{FW})}(x) = u_0 \sum_{m=0}^{M-1}\sum_{j'=-b+1}^{b} \gamma_{m,\bar{n}_m(x)+j'} f_m(2^m(x/\ell) - \bar{n}_m(x) - j'), \tag{14}$$

where $\bar{n}_m(x) \equiv \lfloor 2^m(x/\ell)\rfloor$, and the notation $\lfloor y\rfloor$ denotes the greatest integer not exceeding the real value y. To implement this formula numerically, one need only specify how the independent standard Gaussian random variables γ_{mj} are to be generated. At least two different approaches can be adopted, as we will discuss in Section 5.1.3.3.

Detailed analysis of the errors of interpolation, discretization, and aliasing in the evaluation of the Fourier transform (10) can be found in [6]. In our simulations, we shall simply use the numerical parameters p, b, and $\Delta\xi$ which were found to work well in [6].

We will focus our attention on the cost of the Fourier-wavelet method (Section 5) and the quality of the random field statistics which it generates (Sections 6 and 7), particularly in comparison to the Randomization method. The Fourier-wavelet method is somewhat more complicated than the Randomization method, and it does incur a (controllable) statisical bias through truncation of the sums in (14) and the need to approximate the functions f_m through interpolation from a finite set of data points. We will therefore be particularly interested to examine the circumstances in which the extra complexity of the Fourier-wavelet method make it worthwhile relative to the Randomization method.

5. General considerations of cost

We begin our studies of the Randomization and Fourier-wavelet methods by revisiting the question of how much computational effort is required by these methods to generate fractal self-similarity (as measured

by the second order structure function (4)) over a desired number of decades [6,2]. As a point of comparison, we will also briefly discuss their costs relative to a direct Gaussian random field simulation approach which is not adapted for multiscale applications. In neither the Randomization method nor the Fourier-wavelet method does the random field construction make reference to the points at which the random field is to be eventually evaluated. When the evaluation points are irregularly distributed, therefore, the cost of random field construction and evaluation at the desired points does not depend on whether the evaluation points are specified in advance or later on demand. (This is not true of the direct Gaussian random field simulation approach, which we discuss briefly in Section 5.1.1.) Some cost savings can be achieved by the Fourier-wavelet method if the evaluation points are pre-specified and distributed in a regular way, particularly as on a grid covering a specified computational domain. We therefore will begin by discussing the relative computational costs of the Gaussian random field simulation methods in Section 5.1 without any special assumptions on how the evaluation points are distributed, allowing them as well to be specified in advance or on demand. In Section 5.2, we specialize our discussion to the case in which the evaluation points are specified in advance with a regular distribution over a given computational domain. Also included in this special case is the situation where the random field is pre-computed over a regular computational grid, with evaluations at the desired points obtained by a subsequent interpolation step. The results of these cost considerations are summarized in Table 1.

The costs of any of the Gaussian random field simulation methods may be categorized as follows:

- the *preprocessing cost* of taking the desired energy spectrum and making the deterministic calculations needed for the random field representation,
- the *cost in simulating one new realization* of the random field *and evaluating* it at the points desired.

For the Randomization method, the second cost can be cleanly separated into the cost of building a realization of the simulated random field and an additive cost per evaluation. For the Fourier-wavelet method and the direct simulation method, such a decomposition is less clear. Certain aspects of computational cost of the multiscale Gaussian random field simulation algorithms have been considered previously [6,2], but we wish to re-evaluate the cost analysis of the Randomization method in light of new stratified sampling strategies. The preprocessing cost can probably be treated as less important than the other costs if many realizations of a random field with a single energy spectrum are needed [2], but it could play a more important role in dynamical simulations where the energy spectrum evolves in time. We therefore do include a brief consideration of the preprocessing cost.

Our theoretical considerations are intended to apply rather broadly to multiscale random fields in multiple dimensions with characteristic parameters defined in Section 2, but we will refer in our discussion to numerical results for a one-dimensional random field example $u(x)$ with spectral density

$$E(k) = \begin{cases} C_E|k|^{-\alpha}, & |k| \geqslant k_0, \\ 0, & |k| < k_0, \end{cases} \tag{15}$$

with $1 < \alpha < 3$. This random field has correlation length $\ell_c = (\alpha - 1)/(4k_0)$ and $\ell_s = 0$; the latter statement follows formally by introducing a high-wavenumber cutoff and noticing that the expression in (6) vanishes as the cutoff is removed. In numerical calculations throughout the paper we choose specifically $\alpha = 5/3$ (corresponding to the Kolmogorov spectrum for the inertial range of a turbulent flow [14,36,28]), $k_0 = 1$, and $C_E = 1$.

To assess the basic quality of the simulated fractal random fields, we shall use the second order structure function $D(\rho) = \langle [u(x+\rho) - u(x)]^2 \rangle$, where the angle brackets denote an average over an ensemble of independent random field realizations. The second order structure function is related to the spectral density by the formula [48]

$$D(\rho) = \int_0^\infty 4E(k)[1 - \cos(2\pi k\rho)]\, \mathrm{d}k.$$

Note that the main contribution to the structure function $D(\rho)$ at a given value of ρ comes from the wavenumbers which are of order of $1/\rho$. The power law structure of the energy spectrum implies, by Fourier duality,

that the structure function should exhibit a self-similar power law scaling on scales small compared to the cut-off length scale k_0^{-1}:

$$D(\rho) \sim J_\alpha \rho^{\alpha-1} \quad \text{for } \rho \ll k_0^{-1},$$

where

$$J_\alpha = 4C_E \int_0^\infty k^{-\alpha}[1-\cos(2\pi k)]\,\mathrm{d}k = \begin{cases} -\frac{2^{1+\alpha}}{\pi^{1-\alpha}}\Gamma(1-\alpha)\sin(\alpha\pi/2), & 1<\alpha<3,\ \alpha\neq 2, \\ 4\pi^2, & \alpha = 2 \end{cases}$$

and $\Gamma(x)$ for $x<0$ is the Gamma function (extended by analytical continuation) [17,27]. This induced power-law scaling in the structure function is most clearly seen by rewriting the structure function in the form

$$D(\rho) = [J_\alpha - 4\int_0^{\rho k_0}(1-\cos(2\pi k'))k'^{-\alpha}\,\mathrm{d}k']\rho^{\alpha-1}. \tag{16}$$

To display more clearly the accuracy of the simulation methods in replicating the correct scaling (16) of the structure function, we will look at a rescaled form [6]

$$G_2(\rho) = D(\rho)/(J_\alpha \rho^{\alpha-1}),$$

which should satisfy $G_2(\rho) \sim 1$ for $\rho k_0 \ll 1$. We can therefore analyze rather rigorously how well the Monte Carlo methods are simulating the second order statistics of the fractal random field described by spectral density (15) by observing over how many decades the function $G_2(\rho)$ remains near the constant value 1.

As discussed in Section 2, we choose parameters in a random field simulation method based on the maximum and minimum length scales ($\ell_{\max}$, $\ell_{\min}$) of the random field structure which we aim to capture. The crucial determinant of cost is the ratio of these length scales, which we will express in terms of the number of decades separating them:

$$N_{\mathrm{dec}} = \log_{10}(\ell_{\max}/\ell_{\min}).$$

5.1. Random field simulations with evaluations at irregular locations

We begin by considering the cost of simulating a Gaussian random field at a collection of N_e points which may be specified in advance or on demand, and are not assumed to have any regular distribution. We briefly consider the costs of a direct Gaussian simulation scheme (Section 5.1.1), then consider the Randomization method (Section 5.1.2) and the Fourier-wavelet method (Section 5.1.3) in turn.

5.1.1. Direct simulation method

One generic approach to simulating a Gaussian random field at a set of points is to recognize that the values of the random field at these points form a mean zero, jointly Gaussian collection of random variables [48]. The covariance matrix for these Gaussian random variables is obtained from evaluating the correlation function at the relative displacements between each pair of points. If the set of evaluation points is specified in advance, then the simulation task reduces to a preprocessing step of calculating the covariance matrix and its square root (through a Cholesky decomposition), followed by a multiplication of this matrix square root by a vector of standard independent Gaussian random variables for each realization. Performing this procedure for the simulation of the random field at N_e pre-specified points would incur a preprocessing cost which scales as N_e^3 and a cost per realization scaling as N_e^2. The preprocessing step would have to be repeated each time the points of evaluation are changed.

Unlike the multiscale simulation procedures discussed in the present work, the direct simulation procedure must be fundamentally modified if the evaluation points are specified on demand. The value of the random field at each new evaluation point is then given by a Gaussian random variable with mean and variance conditioned upon the values of the random field at the previous evaluation points. (This statement remains true even if the location of the new evaluation point is a random variable depending on the pre-

vious evaluations of the Gaussian random field and possibly some additional independent random variables.) The simulation of the new random field value is therefore equivalent to a standard regression with respect to the previously simulated data [13]. Implementing this regression in a straightforward way would yield a negligible preprocessing cost, and a total cost proportional to N_e^4 to simulate one realization of the values at N_e points specified on demand. The cost is dominated by the calculation of the regression coefficients [13].

We therefore see that in the generic case, the cost of the direct Gaussian random field simulation approach is a superlinear power law in the number of evaluation points N_e. One may be able to reduce the costs of this direct simulation approach somewhat through exploiting information about the particular arrangement of the evaluation points; we consider in particular the case of a regular computational grid in Section 5.2.1.

5.1.2. Randomization method

5.1.2.1. Choice of numerical parameters. In our numerical example (15), we will choose $\ell_{\max} = k_0^{-1}$ (in general it should be comparable to the correlation length ℓ_c). The remaining parameters to be determined are the number of sampling bins, n, and the number of wavenumbers chosen per sampling bin, n_0. These parameters are really set by N_{dec}, the number of decades of accurate simulation desired, as well as our choice of bin widths. We elaborate for each of the variants of the stratified sampling strategy.

Variant A: Without stratified sampling, $n = 1$. Following [2], we can estimate the smallest length scale $\ell_{\min}$ which will be reasonably approximated by the Randomization method using n_0 random wavenumbers as that length scale for which the average number of wave number samples lying in the interval $(1/\ell_{\min}, \infty)$ exceeds some critical numerical value c. The larger we choose c, the more stringently we are interpreting the phrase "accurate representation of the random field down to length scales $\ell_{\min}$".

For our example (15), the average number of wave numbers in the interval $(1/\ell_{\min}, \infty)$ is equal to $n_0(k_0\ell_{\min})^{\alpha-1}$; then from $n_0(k_0\ell_{\min})^{\alpha-1} = c$ we get

$$\ell_{\min} = \frac{1}{k_0}\left(\frac{n_0}{c}\right)^{-\frac{1}{\alpha-1}}. \tag{17}$$

So with n_0 wavenumber samples, the number of decades accurately described is $N_{\text{dec}} = \frac{1}{\alpha-1}\log_{10}(n_0/c)$. Equivalently, the number of wavenumber samples required grows exponentially with the number of decades desired: $n_0 = c10^{N_{\text{dec}}(\alpha-1)}$.

Our calculations show that increasing the number of simulated wavenumbers from $n_0 = 160$ to $n_0 = 1000$ extends the domain of accurate self-similar scaling by less than a decade (see also [2,6]). If we wished to simulate nine decades of scaling, then for $\alpha = 5/3$ we have to sample 10^6 wavenumbers, which is practically unrealistic. Increasing the number of decades of scaling with variant A of the Randomization method therefore requires a very large extra investment of computational effort.

Variant B: Here we select n sampling bins, each with equal energy, and sample n_0 wavenumbers from each bin. Applying similar arguments as in our analysis of variant A, and assuming that the accuracy parameter c is smaller than n_0 (so that $\ell_{\min}$ is assumed to fall in the wavenumber bin with the highest wavenumbers), we obtain

$$c = \frac{n_0 \int_{1/\ell_{\min}}^{\infty} k^{-\alpha}\,\mathrm{d}k}{\frac{1}{n}\int_{k_0}^{\infty} k^{-\alpha}\,\mathrm{d}k}$$

and consequently $\ell_{\min} = \frac{1}{k_0}(nn_0/c)^{-\frac{1}{\alpha-1}}$. The number of decades of accurate scaling is therefore related to our sampling effort as:

$$N_{\text{dec}} = \frac{1}{\alpha-1}\log_{10}(nn_0/c).$$

So the stratification of the sampling into bins of equal energy seems to lead to no improvement in efficiency; the number of decades is again logarithmically related to the total number of wavenumbers nn_0 sampled. The quality of the simulation is also not markedly improved by the equal energy stratified sampling, as seen in Fig. 1.

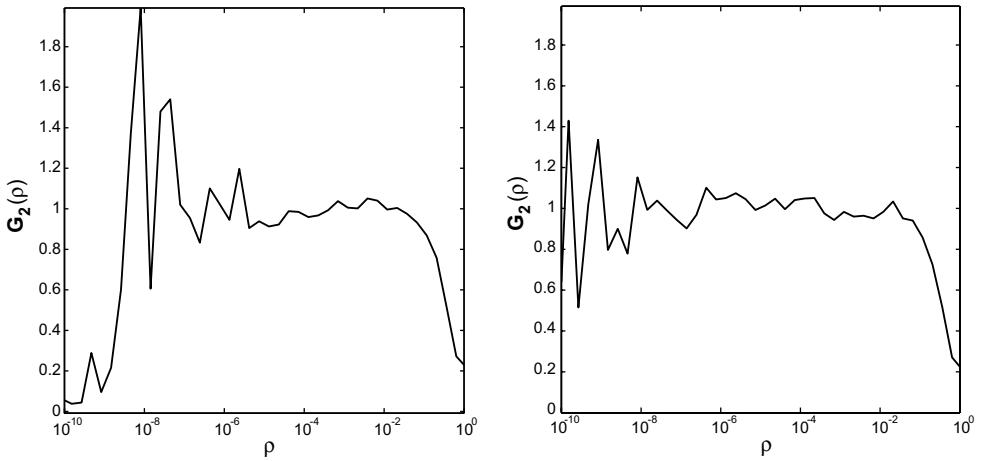

Fig. 1. The normalized structure function $G_2(\rho) = \frac{D(\rho)}{J_{5/3}\rho^{2/3}}$ calculated by variant B of the Randomization method with $N_s = 2000$ samples. Number of sampling bins: $n = 160$ (left panel) and $n = 1000$ (right panel); $n_0 = 1$ wavenumber per bin in both cases.

Variant C: We finally consider how the cost of the logarithmically stratified sampling strategy is related to the range of scales over which one wishes to simulate a multiscale random field accurately. Applying the same criterion as in the previous variants for determining the smallest scale $\ell_{\min}$ which is simulated accurately given the number of sampling bins n, the ratio q between the bin boundaries, and the number of samples n_0 per bin, we obtain $c = n_0(\ell_{\min}\hat{k}_n)^{\alpha-1}$, where $\hat{k}_n = k_0 q^{n-1}$ is the left endpoint of the highest wavenumber sampling bin. Solving for $\ell_{\min}$, we obtain $\ell_{\min} = k_0^{-1} q^{1-n}(n_0/c)^{-1/(\alpha-1)}$, and so the number of decades of accuracy can be estimated as:

$$N_{\text{dec}} = \frac{1}{\alpha - 1}\log_{10}\frac{n_0}{c} + (n-1)\log_{10} q. \tag{18}$$

Note that in contrast to variants A and B of the Randomization method, the number of decades resolved in this case scales linearly with the number of bins n. So if we fix the bin ratio q and the number of samples per bin n_0 at some reasonable values, our theoretical estimate suggests that we can simulate a number of decades proportional to our computational cost by simply increasing the number of sampling bins. This is illustrated by numerical results presented in the left panel of Fig. 2. We see that with the same effort as in the previous

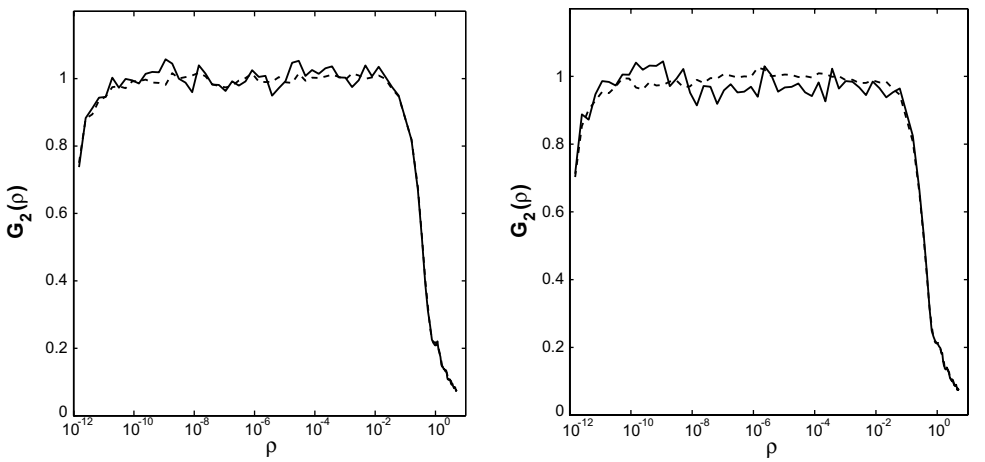

Fig. 2. The normalized structure function $G_2(\rho) = \frac{D(\rho)}{J_{5/3}\rho^{2/3}}$ calculated by: the Randomization method (left panel) with +40 wavenumbers ($n_0 = 1$ sample from each of $n = 40$ bins); and by the Fourier-wavelet method (right panel). Solid lines: $N_s = 2000$ Monte Carlo samples; dashed lines: $N_s = 16{,}000$ samples.

variants of the Randomization method, we are able to simulate nine decades of self-similar scaling accurately. The kurtosis

$$G_4(\rho) = \frac{\langle (u(\rho) - u(0))^4 \rangle}{\langle (u(\rho) - u(0))^2 \rangle^2} \tag{19}$$

is also shown in the left panel of Fig. 3 to be relatively near the desired value +3 throughout the self-similar scaling range, particularly when sufficiently many samples are used.

In these and subsequent numerical calculations with the Randomization Method, we always use the variant C with $n = 40$ bins and bin ratio $q = 2$, except in Fig. 6, where $n = 3$ sampling bins are used. Also, except in Fig. 6, all our numerical calculations use the spectral density (15).

From our exploration of the multiscale random field with spectral density (15), we have found that the Randomization method can be made much more efficient by using stratified sampling schemes other than subdivision into sampling bins of equal energy. We have attempted a logarithmic subdivision strategy because of its natural association with self-similar fractal random fields, using essentially an equal level of resolution at each length scale within the range of the simulation. The Fourier-wavelet method (indeed any wavelet method) employs a similar representation. We do not claim that the logarithmic subdivision strategy is optimal, but only that it appears to improve greatly the efficiency of the Randomization method relative to an equal-energy subdivision. Nor do we take the relation (18) too seriously by, for example, optimizing it with respect to the numerical parameters. This would lead to silly strategies because the formula (18) does not take into account the need to adequately sample wavenumbers *throughout* the range of scales from $\ell_{\min}$ to $\ell_{\max}$. Our rough theoretical considerations are only meant to suggest what to expect with a reasonable choice of parameters to ensure a decent level of accuracy. The main point is that the estimate (18), along with the numerical results in Figs. 2, 3 suggests that the Randomization method with a logarithmic subdivision strategy should be able to simulate a multiscale random field with the number of computational elements growing linearly with the number of decades of random field structure simulated, at least insofar as producing an accurate simulated structure function and kurtosis. We expect this cost scaling to apply to more general multiscale random fields as well. Results of simulation with the Fourier-wavelet Method with $M = 40$ and $b = 10$ are shown in the right panels of Figs. 2 and 3 for comparison. From Fig. 2, we see that the choice of $n_0 = 1$ harmonics per bin in the Randomization method yields approximately the same accuracy in the structure function as that of the Fourier-wavelet method. Fig. 4 shows that increasing n_0 does not lead to a significant decrease of the error. For higher statistical moments like kurtosis, however, the error of the Randomization method with $n_0 = 1$ is considerably larger than that of the Fourier-wavelet method (Fig. 3). An increase in the number of harmonics per bin $n_0 = 4$ is needed for comparable accuracy (with $N_s = 2000$ Monte Carlo samples) with the Fourier-wavelet

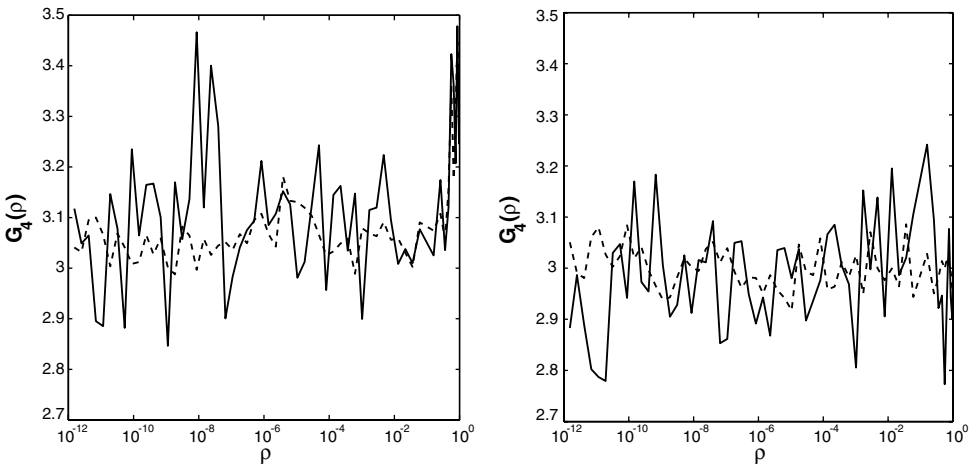

Fig. 3. Kurtosis $G_4(\rho)$ calculated by: the Randomization method (left panel) with 40 wavenumbers ($n_0 = 1$ samples from each of $n = 40$ bins); and by the Fourier-wavelet method (right panel). Solid lines: $N_s = 2000$ Monte Carlo samples; dashed lines: $N_s = 16{,}000$ samples.

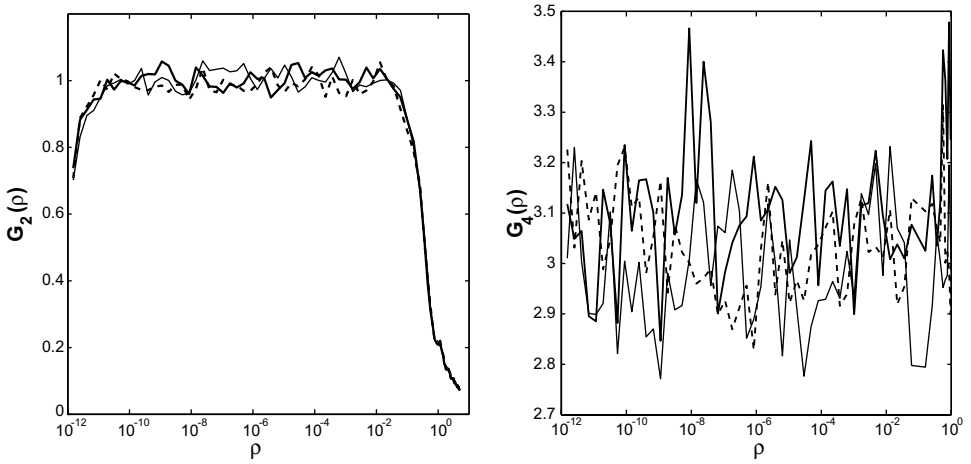

Fig. 4. The normalized structure function $G_2(\rho)$ (left panel) and kurtosis $G_4(\rho)$ (right panel) calculated by Randomization method for different values of the number of harmonics n_0 per sampling bin: $n_0 = 1$ (bold line), $n_0 = 4$ (dashed line), and $n_0 = 10$ (thin line). All results here are for $N_s = 2000$ Monte Carlo samples.

method (Fig. 4, right panel). A further increase to $n_0 = 10$ is seen in this figure not to improve significantly the simulated kurtosis.

In summary, we see that in order to simulate a random field for the purposes of evaluation at an irregularly situated set of points, we expect that a Randomization method with logarithmic subdivision strategy could be adequate with some fixed reasonable bin ratio (such as $q = 2$), some fixed reasonable number of wavenumbers sampled per bin (such as $n_0 \sim 4$–10), and the number of sampling bins n chosen in proportion to the number of decades of random field structure to be simulated (so proportional to $\log_{10}(\ell_c/\ell_s)$ if the full structure of the random field is to be represented). We emphasize that, based on the results presented so far, we can only expect these choices of parameters to be adequate insofar as accurate simulation of two-point statistics (such as the structure function (4) and two-point kurtosis (19)) evaluated at arbitrary points suffices for the application. In Sections 6 and 7, we examine how well the Randomization method is able to recover multi-point statistical properties.

5.1.2.2. Preprocessing cost. The Randomization method has a preprocessing cost proportional to the number of stratified sampling bins n.

For subdivision strategies which are determined without detailed computation involving the energy spectrum (such as variant C), one needs to prepare a transform or rejection method in each bin to convert a standard uniform random number to the correct probability distribution of wavenumbers within each sampling bin. For bins set by equal energy distribution (variant B), one must also compute where the bin divisions lie. We will not concern ourselves with quantifying this additional cost because the equal energy distribution strategy does not seem to have an advantage (compared to, say, variant C) justifying the extra computation.

5.1.2.3. Cost per realization. A new random field is simulated by choosing n_0 wavenumbers randomly within each of the n bins, and then generating a Gaussian random amplitude for each of these wavenumbers. The cost is proportional to a small multiple of $n_0 n$. The evaluation of the simulated random field at each desired point is accomplished by straightforward summation of the Fourier series approximation (8), with a cost proportional to nn_0, the number of terms in the sum. Therefore, the total cost in generating a realization of the random field at N_e irregularly spaced points scales as $N_e n_0 n$.

5.1.2.4. Summary of cost considerations. The preprocessing cost is proportional to the number of sampling bins n, while the cost per realization is proportional to the total number of wavenumbers sampled and number of evaluations, $n_0 n N_e$. Each of these costs are expected to scale linearly with the number of decades of random field structure to be simulated, at least if accuracy of the simulated second-order statistics is all that is required.

Similar conclusions about the cost hold in multi-dimensional implementations of the Randomization method [42]; the main difference is that the number of harmonics per sampling bin n_0 will typically need to increase as a function of dimension (but not with respect to the ratio of any length scales).

5.1.3. Fourier-wavelet method

5.1.3.1. Choice of numerical parameters. As with the Randomization method, one must choose the maximal and minimal length scales, $\ell_{\max}$ and $\ell_{\min}$, to be resolved by the random field simulation. The maximal length scale $\ell_{\max}$ is generally taken to be comparable to the correlation length of the random field; in our example (15), we choose $\ell_{\max} = k_0 = 1$. The ratio between the minimal and maximal length scales is set by the choice of the number of scales M in the truncated random field representation (14), namely $(\ell_{\max}/\ell_{\min}) = 2^{M-1}$. The number of decades which one is attempting to capture is

$$N_{\text{dec}} = \log_{10}(\ell_{\max}/\ell_{\min}) = (M-1)\log_{10}2.$$

Good statistical quality will generally be somewhat less than this ideal figure, but we should expect the number of decades for which the random field will be accurately simulated to scale linearly with $M-1$.

One must additionally choose the truncation parameter b to be large enough that the functions $f_m(\xi)$ derived from the wavelets can be considered negligible for $|\xi| > b$. Generally speaking, $f_m(\xi)$ decays algebraically, with power law $|\xi|^{-p}$ if the Meyer mother wavelet is built out of a pth order perfect B-spline [6]. The values of p and b primarily affect the relative error of the statistics of the simulated random field (arising from the truncation of the sum over translates in (14)), and in general need not be adjusted when simulating random fields with various length scales, so long as the relative accuracy required remains fixed. Following [6], we choose $p = 2$ and $b = 10$.

Finally, we must choose a finite spacing $\Delta\xi$ between the points $\xi = \xi_j = -b + (j-1)\Delta\xi, j = 1, \ldots, 2b/\Delta\xi + 1$ at which the functions $f_m(\xi)$ are numerically evaluated through their Fourier integrals (10). We will assume that $1/\Delta\xi$ is an integer. The choice of $\Delta\xi$ determines how accurately the functions f_m are approximated through interpolation from the computed values throughout the interval $|\xi| \leqslant b$ over which they may need to be evaluated in the representation (14). Like b and p, the numerical value $\Delta\xi$ is determined by the amount of bias due to numerical discretization which is tolerable in the statistics, and is insensitive to the length scales characterizing the random field to be simulated, since the functions $f_m(\xi)$ are each single-scale functions. The value $\Delta\xi = 0.01$ was used in our calculations.

An example of the normalized structure function $G_2(\rho)$ and the kurtosis $G_4(\rho)$ for the energy spectrum (15) as simulated by the Fourier-wavelet method with $M = 40$ scales and $b = 10$ is shown in the right panels of Figs. 2 and 3. In subsequent numerical examples, we continue to use these simulation parameters and energy spectrum, except in Fig. 6, where energy spectrum (22) is used.

5.1.3.2. Preprocessing cost. Once the numerical parameters have been chosen, the functions f_m used to represent the random field on various length scales each need to be computed through evaluation of the Fourier transforms (10). Some details of how these values can be calculated through a fast Fourier transform are given in Appendix A. The cost of each integration is $(b/\Delta\xi)\log_2(b/\Delta\xi)$ and M functions f_m need to be computed. Since these numerical integrations dominate the preprocessing cost, we can estimate it as $M(b/\Delta\xi)\log_2(b/\Delta\xi)$.

5.1.3.3. Cost per realization. One key observation that distinguishes the Fourier-wavelet method from the Randomization method as well as the direct simulation method discussed in Section 5.1.1 is that the evaluation of random field at a point does not involve a summation over all the computational elements and associated random numbers. Rather, because of the good localization properties of the wavelet basis, one need only sum at each scale over a fixed number $(2b)$ of wavelets which are situated closest to the point of evaluation. Consequently, one has two options with the Fourier-wavelet method:

- Simulate at the beginning of the calculation the complete random field representation over the whole computational domain, then evaluate this random field representation at the desired locations.
- Simulate the random field only as needed to evaluate its values at the desired points of interest.

The execution and accounting is simpler for the first approach, which we now discuss, though it requires the ability to store a large number of random variables. Later we will remark on how one may be able to reduce computational cost and memory requirements through the second approach, particularly if the number of points at which the random field is to be evaluated are sparsely distributed over the simulation domain.

Pre-computation of all random variables: We can estimate the amount of work needed to pre-compute all coefficients needed for evaluations on a one-dimensional domain of length L by first fixing an index $0 \leqslant m \leqslant M$ (which fixes a length scale $\ell 2^{-m}$), and noting that we must simulate and store γ_{mj} for $2^m L/\ell + 2b$ different indices j in (9), so that the sum (14) can be accurately evaluated at any value of x in the domain. This follows from counting the number of integers j such that $|\bar{n}_m(x) - j| \leqslant b$ for some x within an interval of length L. Consequently, the cost to simulate one realization of all coefficients of the one-dimensional random field representation comprehensively (to the specified level of accuracy) over a domain of length L is

$$\sum_{m=0}^{M-1}(2^m L/\ell + 2b) \approx 2^M L/\ell + 2bM.$$

The evaluation of the random field at a given point involves the calculation of a sum of the form (14). This involves interpolation to evaluate the functions f_m at the indicated values, and a summation over the indicated wavelets with their associated random numbers (already simulated). The cost of this evaluation step is proportional to bMN_e.

Consequently, the total cost for simulating one realization of the random field at a set of N_e irregularly situated points should scale as $2^M L/\ell + bMN_e$ if all random variables in the random field representation are calculated in advance of evaluation at the desired points.

Evaluation of random variables as needed: One can cut the memory and run-time costs if the random variables in the Fourier-wavelet random field representation are only simulated as needed for evaluation [10,9,8]. The cost savings would be most dramatic in a situation where the random field is to be evaluated over a sparsely distributed set of points (which may still be large in number). In particular, one can apply this approach without specifying the computational domain in advance. In this strategy, however, one must be careful with managing the random numbers γ_{mj} so that the same values are used when the same indices are referred to in random field evaluations at different locations x. One can either store all random numbers that have been generated and develop an efficient data handling routine to check whether a random variable γ_{mj} appearing in an evaluation needs to be generated or recalled from a previous generation. Alternatively, one can use explicitly the structure of a reversible pseudo-random number generator to simulate all random variables as needed, maintaining the identities of random variables already realized, without actually storing them [8]. In short, one may be able to save on computation time by only simulating the random field as needed, but one must adopt a more sophisticated code to handle the random numbers γ_{mj}. The run-time cost of simulating the random field at an irregularly situated set of N_e points should then simply scale with the cost of evaluating the sums (14), which scales as $N_e bM$.

5.1.3.4. Summary of cost considerations. The preprocessing cost of the Fourier-wavelet method is proportional to the quantity $M(b/\Delta\xi)\log_2(b/\Delta\xi)$, while the cost per realization over an irregularly distributed set of N_e points is proportional to $2^M L/\ell + bMN_e$ if all random variables in the random field representation are computed in advance of evaluation, or simply proportional to MbN_e if the random variables are simulated only as needed and managed by a sufficiently sophisticated algorithm. The preprocessing cost appears negligible relative to the cost per realization when N_e is large. We recall that the number of scales M in the Fourier-wavelet representation is related to the range of scales in the random field by $\ell_{\max}/\ell_{\min} = 2^{M-1}$.

In the multi-dimensional extension of the Fourier-wavelet method through superposition of one-dimensional plane waves [9], the main change in the cost will be an overall dimension-dependent factor in the cost per realization representing the number of plane waves needed.

5.1.4. Comparison of costs

We only consider the most competitive variant C, with logarithmically uniform subdivision, of the Randomization method. For this Randomization method, the computational cost per realization is found rather

simply to be proportional to the number of decades resolved in the random field and the number of points to be evaluated. The prefactor in the cost is determined by the number of wavenumbers that should be simulated per decade to provide sufficient statistical accuracy. To simulate statistics involving a small number of points accurately, this prefactor is on the order of 10.

The cost of simulating a multiscale Gaussian random field with the Fourier-wavelet method appears usually to be greater. If the random variables in the Fourier-wavelet representation are simulated only as needed for evaluation, the cost scales nominally with $bN_e\log_2(\ell_{\max}/\ell_{\min})$. This may be viewed as ostensibly comparable to the cost scaling in the Randomization method, but one must recall that to achieve such cost scaling in the Fourier-wavelet method for $N_e > 1$, the code must involve a somewhat sophisticated handling of the random numbers γ_{mj} in the expansion (9), thereby increasing the amount of work per calculation.

If one wishes to avoid the need for a delicate management of random variables in the Fourier-wavelet method, and one can pre-specify a bounded domain in which the points to be evaluated must lie, then one can simulate the random field over the whole domain, before evaluation, in which case the cost will generally scale as $L/\ell_{\min} + bN_e\log_2(\ell_{\max}/\ell_{\min})$. The first term has the potential for growing quite large for random fields with many scales, and has no counterpart in variant C of the Randomization method.

Both the Randomization and Fourier-wavelet methods are much less expensive than the standard simulation approach described in Section 5.1.1 when a multiscale random field (with $\ell_c/\ell_{\min} \gg 1$ and $L/\ell_{\min} \gg 1$) is to be evaluated at a large number N_e of points. Indeed, the cost of the Randomization method scales linearly in N_e, logarithmically with respect to $\ell_c/\ell_{\min}$, and is independent of $L/\ell_{\min}$. The Fourier-wavelet method has similar cost scaling with careful random variable management, but even with the simpler approach of precomputing all random variables associated to the computational domain, the cost of the Fourier-wavelet method scales as $L/\ell_{\min} + bN_e\log_2(\ell_c/\ell_{\min})$, which scales logarithmically with respect to $\ell_c/\ell_{\min}$ and linearly (and additively) with respect to $L/\ell_{\min}$ and N_e. The standard simulation method described in Section 5.1.1, by contrast, has cost scaling superlinearly with respect to N_e.

We observe, then, that the Randomization method with logarithmically uniform subdivision can be expected to simulate a random field with accurate two-point statistics with less expense than the Fourier-wavelet method. The reason for the reduced cost of the Randomization method is easily traced to its use of a smaller set of computational elements. To simulate the random field structure at each length scale $2^{-m}\ell_{\max}$, the Randomization method uses a fixed number n_0 of wavenumbers, while the Fourier-wavelet method uses an increasing number $2^mL/\ell_{\max} + 2b$ of wavelets at smaller scales (larger m). The Randomization method has the flexibility in design in allowing the number of wavenumbers per sampling bin n_0 and therefore the number n_0n of computational elements to be chosen according to the statistical accuracy requirements. The Fourier-wavelet method, by contrast, really requires reference to a complete set of $\sum_{m=0}^{M-1}(2^mL/\ell_{\max} + 2b) \approx 2^ML/\ell_{\max} + 2Mb = 2(L/\ell_{\min} + b\log_2(\ell_{\max}/\ell_{\min}))$ wavelets and associated random numbers to represent the random field meaningfully. The numerical parameters governing statistical accuracy in the Fourier-wavelet method relate to the number of terms used in evaluating the random field at a given location.

We remark that the standard approach described in Section 5.1 would require L/h random variables to represent the random field over a domain of length L with computational grid spacing h. The Fourier-wavelet method would use approximately the same number of random variables if $h \geqslant \ell_s$, so that the random field has structure all the way down to the grid scale and $\ell_{\min} = h$. If $h < \frac{1}{2}\ell_s$, then the Fourier-wavelet method would be using a smaller number of computational elements than the direct approach because the random field structure on length scales smaller than ℓ_s can be obtained accurately by interpolation (without the need for additional random numbers) from the smoothness length scale ℓ_s of the random field. The Fourier-wavelet method, therefore, has the number of computational elements (and associated random variables) set essentially by theoretical considerations of how many degrees of freedom of randomness are needed to represent effectively a random field over a computational domain.

The Randomization method, by contrast, has the number of its random variables and computational elements (wavenumbers) set by user specification. In particular, in an accurate simulation over nine decades of the second order structure function of the random field described by (16), the Randomization method (with $n = 40$, $n_0 = 1$) uses only $120 = 3 \times 40$ random variables to represent the random field while the Fourier-wavelet method makes reference, in principle, to as many as 2^{42} random variables. Apparently, the smaller number of random variables is sufficient for the random field simulated by the Randomization method to exhibit a

good fidelity in the second order structure function as well as the kurtosis of the random field increment between two points (19). An interesting question is to what extent the Randomization method can exploit its flexibility in design and use of a relatively small number of computational elements and random variables to represent the random field over a computational domain when more complex statistics of the random field are important.

We will see through numerical examples in the next few sections that the Randomization method must increase the number of wavenumbers n_0 simulated per scale as accuracy is desired in statistical characteristics involving a greater number of points. (We have already seen an increase of n_0 from 1 to 4 is necessary for adequate behavior of the two-point kurtosis (Fig. 4).) By contrast, the Fourier-wavelet method appears to simulate multi-point statistics accurately with the same choice of parameters as was used to simulate the second order structure function accurately (Figs. 7 and 8). We will find that the Randomization method remains competitive for the simulation of statistics involving tens of points, but that the Fourier-wavelet method might become more efficient in simulating statistics involving a greater number of points. In particular, the Fourier-wavelet method is more efficient in simulating a random field with good ergodic properties (so that spatial averages over the whole domain approximate ensemble statistics).

We remark that the other variants (A and B) of the Randomization method would have costs growing faster than that of the Fourier-wavelet method for multiscale random fields with many decades; it is important to use the logarithmically uniform subdivision to render the Randomization method competitive for such applications. Alternatively, one could also consider the simulation method of [2], which is a hybrid of the standard Fourier method with variant B of the Randomization method. The number of decades which can be simulated by the hybrid method grows only logarithmically with cost, just like variants A and B of the Randomization method, but by suitable choice of parameters the scaling prefactors can be made small enough so the method is competitive with the Fourier-wavelet method for simulating fields with up to 9–11 decades of self-similar scaling of the structure function. As we have discussed above, variant C of the Randomization method appears to have a lower prefactor relative to the Fourier-wavelet method in the linear scaling of cost with respect to number of decades simulated, which would imply that variant C of the Randomization method will become more efficient than the hybrid method after a smaller number of decades. We remark that the ability of the hybrid method to simulate multi-point statistics accurately and exhibit good ergodic properties have not yet been explored, as they will be for the Randomization and Fourier-wavelet methods in Sections 6 and 7.

5.2. Random field simulations on regular grid over pre-specified domain

We now discuss the relative costs of the Randomization and Fourier-wavelet methods, as well as the direct simulation approach, when the random field is to be simulated on a pre-specified regular grid of points in one dimension with spacing h and domain length L. The arguments extend directly to d-dimensional domains described by a single length scale L and grid configuration which covers the domain with spacing between neighbors characterized by a single length scale h, provided factors (L/h) and (ℓ_c/h) are replaced by $(L/h)^d$ and $(\ell_c/h)^d$, respectively. In this subsection, we only point out how the cost scalings change and compare in a relative sense due to the regular arrangement of evaluation points. This discussion is also intended to cover the case in which the random field is to be evaluated at a dense set of irregularly spaced points through pre-computation over a regular grid followed by interpolation. Our considerations of course apply to the pre-computation over the regular grid; the subsequent interpolation is independent of the random field simulation algorithm and is clearly linear in the number of evaluation points.

5.2.1. Direct simulation method

As discussed in Section 5.1.1, one can use Cholesky decomposition to simulate a Gaussian random field on a pre-specified set of points. The number of points at which the random field is to be evaluated on the computational grid scales with L/h, so the preprocessing cost from a naive implementation would scale as $(L/h)^3$, and the cost to simulate one realization of the random field over the grid would scale as $(L/h)^2$.

However, when the domain length L is large compared with the largest resolved length scale $\ell_{\max}$ of the random field, one can easily reduce the cost by neglecting the correlations between points separated by a distance large compared with the $\ell_{\max}$. This gives the covariance matrix a banded structure, reducing the compu-

tational linear algebra costs so that the preprocessing cost scales with $(L/h)(\ell_{\max}/h)^2$ and the cost per realization scales as $(L/h)(\ell_{\max}/h)$.

5.2.2. Randomization method

The cost considerations for the Randomization method are essentially unchanged. The preprocessing cost scales with the number of sampling bins n_0, and then each realization of the random field over the L/h lattice points requires a number of computations proportional to nn_0L/h. We recall for variant C, with logarithmically uniform stratified sampling, the number of decades simulated is proportional to n. There does not appear to be any cost savings available from the evaluation points falling on a regular lattice; the fast Fourier transform is not available due to the irregular spacing of the wavenumbers used in the Randomization method.

5.2.3. Fourier-wavelet method

To a first approximation, we can relate the cost for simulating a random field over a regular lattice by simply viewing it as a special case of making $N_e = L/h$ evaluations of the random field over a domain with length scale L. In this case, it is clearly more efficient to simulate directly all the random variables γ_{mj} needed, so long as they can be stored. We therefore estimate a preprocessing cost proportional to $Mb/\Delta\xi\log_2(b/\Delta\xi)$, and a cost of simulating each realization of the random field over the prescribed lattice proportional to $2^M L/\ell + bML/h$. Fast wavelet transform methods (filter bank algorithms) [30] have the potential of reducing the cost even more, in analogy to fast Fourier transforms, but we are unaware of any actual implementations in the random field context. It is natural to take the sampling distance h comparable to the smallest length scale $\ell_{\min} = \ell 2^{1-M}$ resolved in the Fourier-wavelet representation, in which case we can re-express the cost per realization of the random field on the lattice as proportional to $L/h + bML/h \sim bML/h$. The cost scaling would be the same if the random variables were computed only as needed, and the random variable management would be considerably easier for evaluation on a regular computational grid than in the case of irregularly distributed points (as discussed in Section 5.1.3).

5.2.4. Comparison of costs

With the dense sampling of the random field implicit in simulating the random field over a regular lattice, both the Randomization method and Fourier-wavelet method scale similarly with respect to the length scales involved. Namely, they are both proportional to the number of lattice points L/h, the number of decades simulated (which is logarithmic in $\ell_{\max}/h$), and some numerical implementation parameters. The numerical prefactors appear to be smaller for the Randomization method. In particular, a 2.5%-accuracy could be achieved by the Randomization method ($n = 40$, $n_0 = 1$, $q = 2$) over nine decades of the simulated structure function with approximately 12 times less computer time than the Fourier-wavelet method with parameters ($M = 40$, $b = 10$) specified as in [6] (see Fig. 2, dashed lines). The structure function was evaluated over a complete regular spatial grid by the dependent sampling technique. Both the Randomization and Fourier-wavelet methods are again much more efficient than the standard simulation approach based on Cholesky decomposition of the covariance matrix associated to the pre-specified grid for multiscale applications ($L/h \gg 1$ and $\ell_{\max}/h \gg 1$), since the latter has cost scaling as a superlinear power law with respect to these large parameters. A summary of the costs of the various random simulation methods for both irregularly and regularly distributed evaluation points is presented in Table 1.

We conclude our theoretical cost considerations with a brief discussion about the expected relative costs of the methods in partially regular situations, where the evaluation points are not distributed over a regular computational grid but do have some spatial structure that can be exploited to reduce computational costs from the generic irregularly distributed case discussed in Section 5.1. We interpolate our conclusions from the estimates for the irregularly and regularly distributed cases discussed above. The direct simulation approach should generally have cost scaling as a superlinear power law in N_e, L/h, and $\ell_{\max}/h$. The Randomization and Fourier-wavelet methods, by contrast, should have costs scaling linearly in N_e and logarithmically in $\ell_{\max}/h$. This cost-scaling for the Fourier-wavelet method applies when the random variables in its random field representation are only computed as needed (and therefore managed in a careful way). A simpler implementation of the Fourier-wavelet method in which all the random variables are pre-computed and stored will have a cost scaling linearly with N_e and L/h, and logarithmically with $\ell_{\max}/\ell_{\min}$, the ratio of the maximal and min-

Table 1
Cost scalings of random field simulation methods (DSM = direct simulation method, RM = randomization method (variant C), FWM = Fourier wavelet method, RV = random variable) with respect to largest ($\ell_{\max}$) and smallest ($\ell_{\min}$) resolved scales, length scale of domain L, number of realizations N_s, number of evaluation points per realization N_e, and for evaluation on a one-dimensional regular grid, the length scale h at which the random field is sampled

	Evaluation point configuration	
	Irregular locations	Regular grid
DSM	$N_e^3 + N_s N_e^2$ or $N_s N_e^4$	$(\frac{L}{h})(\frac{\ell_{\max}}{h})^2 + N_s(\frac{L}{h})(\frac{\ell_{\max}}{h})$
RM	$N_s N_e n_0 \log_2(\frac{\ell_{\max}}{\ell_{\min}})$	$N_s n_0(\frac{L}{h})\log_2(\frac{\ell_{\max}}{\ell_{\min}})$
FWM (precomputed RV)	$\log_2(\frac{\ell_{\max}}{\ell_{\min}})(\frac{b}{\Delta\xi})\log_2(\frac{b}{\Delta\xi}) + N_s[\frac{L}{\ell_{\min}} + N_e b\log_2(\frac{\ell_{\max}}{\ell_{\min}})]$	$\log_2(\frac{\ell_{\max}}{\ell_{\min}})(\frac{b}{\Delta\xi})\log_2(\frac{b}{\Delta\xi}) + N_s b(\frac{L}{h})\log_2(\frac{\ell_{\max}}{\ell_{\min}})$
FWM (RV as needed)	$\log_2(\frac{\ell_{\max}}{\ell_{\min}})(\frac{b}{\Delta\xi})\log_2(\frac{b}{\Delta\xi}) + N_s N_e b\log_2(\frac{\ell_{\max}}{\ell_{\min}})$	$\log_2(\frac{\ell_{\max}}{\ell_{\min}})(\frac{b}{\Delta\xi})\log_2(\frac{b}{\Delta\xi}) + N_s b(\frac{L}{h})\log_2(\frac{\ell_{\max}}{\ell_{\min}})$

Other parameters appearing in the expressions (n_0 for the Randomization method; b and $\Delta\xi$ for the Fourier-wavelet method) are quantities which are generally of order 1–10 and held fixed for a given level of desired accuracy, independently of the physical and resolution length scales. Their precise meanings are explained in the main text. The cost scaling estimates in the table (as well as in the main text) generally omit numerical constants independent of parameters; they are only meant to indicate scaling properties and not precise absolute magnitudes.

imal scales of the simulated random field. This would generally be considerably more expensive than the Randomization method except in situations where the number of evaluation points N_e is comparable to L/h (as for the case of a regular computational grid). Finally, both the Randomization method and Fourier-wavelet method are more efficient than the direct simulation method when simulating a multiscale random field ($\ell_{\max}/h \gg 1$) at a large number of points $N_e \gg 1$, because the direct approach has cost scaling as a superlinear power law with respect to these parameters, while the multiscale methods scale as products of linear and logarithmic functions of these parameters.

6. Ergodic properties of simulated random fields

An important feature of numerically simulated statistically homogenous random fields is the quality of their ergodicity, by which is meant the convergence of spatial averages of quantities to their theoretical averages taken over a statistical ensemble. Ergodicity is a particularly useful feature of a simulated random field when each realization is expensive to compute, because statistics can be extracted by processing spatial averages of one or a small number of realizations instead of by averaging over a large set of realizations. Simulation of a porous medium flow through the Darcy equation (2) for a given realization of the conductivity, for example, is a rather time-consuming computational procedure. Computation of statistical flow properties through spatial rather than ensemble averages would therefore improve efficiency if they could be calculated accurately.

As a basic example, we consider the second order correlation function and structure function of the random field, which have, respectively, the theoretical ensemble-averaged definitions:

$$B(\rho) = \langle u(\rho + x)u(x)\rangle, \quad D(\rho) = \langle (u(\rho + x) - u(x))^2\rangle. \tag{20}$$

Neither depend on x due to statistical homogeneity. Rather than considering the quality of ensemble averages (as we did in Section 5), we now study how well corresponding spatial averages of a *single realization* of the simulated random field:

$$\begin{aligned} B_{N_b}(\rho) &\equiv \frac{1}{N_b}\sum_{j=1}^{N_b} u(\rho + (j-1)\ell_b)u((j-1)\ell_b), \\ D_{N_b}(\rho) &\equiv \frac{1}{N_b}\sum_{j=1}^{N_b} [u(\rho + (j-1)\ell_b) - u((j-1)\ell_b)]^2 \end{aligned} \tag{21}$$

converge to the ensemble-averaged expressions $B(\rho)$ and $D(\rho)$ as the number of spatial samples N_b is taken large. Here ℓ_b is a length scale describing the spatial translation between each spatial sample. For efficient convergence of the spatial averages (21) to the ensemble averages (20) as N_b increases, we choose ℓ_b large en-

ough so that the terms in (21) become independent or at least weakly dependent. In our calculations, we take $\ell_b = 2\ell_{\max}$.

To study the ergodicity properties of the simulated random fields, we compare simulated spatial averages for the correlation function and the normalized structure function $G_2(\rho) = D(\rho)/(J_\alpha \rho^{\alpha-1})$ against the exact results for the energy spectrum (15).

6.1. Randomization method

In Fig. 5, these comparisons are made for variant C of the Randomization method. Note that even for $N_b = 16{,}000$ spatial samples, $n = 40$ bins, and $n_0 = 10$ wavenumbers per bin, the agreement is not satisfactory (left panel). Increasing n_0, the number of wavenumbers per bin, improves the results (right panel).

Thus we see that the number of wavenumbers per bin must be drastically increased for the Randomization method to exhibit good ergodic properties. This phenomenon actually arises also for single-scale random fields. To show this, we simulate a random field with the spectral function

$$E(k) = \begin{cases} C_E |k|^{-\alpha}, & k_0 \leqslant |k| \leqslant k_{\max}, \\ 0, & \text{otherwise} \end{cases} \tag{22}$$

with $\alpha = 5/3, C_E = 1$, $k_0 = 1$, and $k_{\max} = 8$. We present spatially averaged statistics from a Randomization method simulation of the random field with this spectral function (22) in Fig. 6,. Here the bins are constructed by subdividing the wavenumber range $k_0 < k < k_{\max}$ into $n = 3$ logarithmically uniform subintervals. In the left panel, $n_0 = 10$ random wavenumbers are sampled in each bin; note that even averages over $N_b = 16{,}000$ spatial blocks exhibit large deviations from the true statistics. Increasing the number of wavenumbers per bin to $n_0 = 200$ (see the right panel) improves the results.

We see that achieving good ergodic properties in the random fields simulated by the Randomization method requires a substantial increase in the number of wavenumbers sampled per bin and therefore the expense of the simulation.

6.2. Fourier-wavelet method

In Fig. 5, right panel, the normalized structure function as estimated by spatial averages of random fields simulated by a single realization of the Fourier-wavelet method is compared against the exact result for the

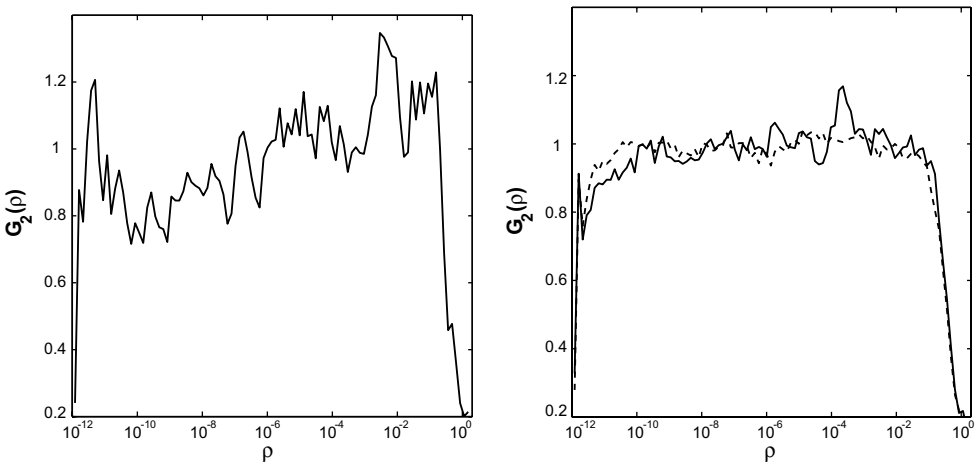

Fig. 5. The normalized structure function $G_2(\rho)$ obtained by ergodic averaging over spatial translations (21) with $N_b = 16{,}000$ and $\ell_b = 2\ell_{\max}$. Left panel: Randomization method with $n_0 = 10$ wavenumbers per bin. Right panel: Randomization method with $n_0 = 100$ (solid line), and Fourier-wavelet method (dashed line).

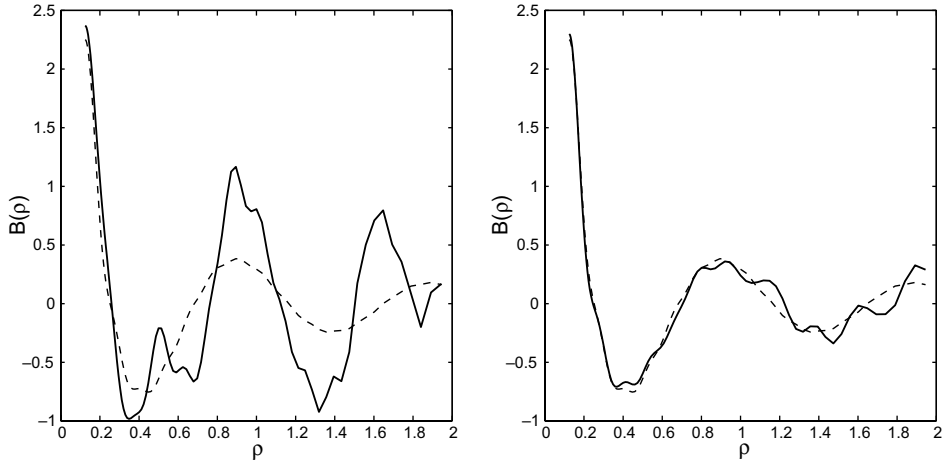

Fig. 6. Ergodic averaging for the correlation function $B(\rho)$ with spectral function (22) over $N_b = 16{,}000$ spatial blocks using the Randomization method with $n = 3$ sampling bins, $k_0 = 1$, $k_{\max} = 8$, bin ratio $q = 2$, and $\ell_b = 2\ell_{\max}$. In the left panel $n_0 = 10$, and in the right panel $n_0 = 200$. The dashed line denotes the exact correlation function corresponding to the spectral function (22), while the bold solid line denotes the simulated average over spatial translations (21).

Kolmogorov spectrum (15). With $N_b = 16{,}000$ spatial blocks, the accuracy achieved was higher than that of the Randomization method with $N_b = 16{,}000$ spatial blocks, $n = 40$, and $n_0 = 100$; see Fig. 5.

6.3. Comparison

We see that in order for computed spatial averages to approximate the desired correlation function or structure function, the Randomization method requires a drastic increase in the number of wavenumbers per bin, n_0, as compared to the values of n_0 adequate for ensemble average calculations. This can be understood by noting that the statistical quality of ergodic averages over a large spatial domain is related to the number of effectively independent samples in the collection of spatial observations. The Randomization method with logarithmically uniform stratified sampling uses a relatively small number of independent random numbers to generate the random field, and spatial averages will fail to improve once they already involve a number of effectively independent samples comparable to the number of independent random numbers $3nn_0$ used in the construction of the random field. The Fourier-wavelet method, by contrast, involves a sufficiently rich collection of random variables so that spatial averages exhibit good ergodic properties without the need to increase the expense of the simulation beyond that necessary for ensemble averages to approximate the second order correlation function and structure function adequately. In our numerical example, the Randomization method required more than 15 times the computational time ($n = 40$, $n_0 = 200$) as the Fourier-wavelet method (with $M = 40$ and $b = 10$) to achieve comparable accuracy over nine decades in the structure function when calculated using spatial averages of a single realization.

7. Multi-point statistical characteristics of simulated random fields

We now return to consideration of the quality of ensemble averages in multiscale random field simulations, but now examine the quality of statistics involving more than two points. One aim is to examine whether the non-Gaussianity of the Randomization method may exhibit itself in a more pronounced manner in multi-point statistics as compared to two-point statistics (such as the second order correlation function and structure function). Another objective is to determine whether the cost of the Randomization method must be increased (as it was for spatial averages) in order to simulate multi-point statistics through ensemble averaging with comparable quality to that simulated by the theoretically Gaussian Fourier-wavelet method. We remark that the consideration of spatial averages (21) in Section 6 yields a statistic that involves more than two points, but we only considered single realizations rather than ensemble averages of these random variables.

We therefore consider the following sequence of normalized random increments

$$\Delta u_i = \frac{u(ih) - u((i-1)h)}{[J_\alpha h^{\alpha-1}]^{1/2}}, \quad \delta u_i = \frac{u(hq_0^{i-1}) - u(0)}{[J_\alpha (hq_0^{i-1})^{\alpha-1}]^{1/2}}, \quad i = 1, \ldots, n'. \tag{23}$$

and the associated random variables

$$\zeta_k = \max_{1 \leqslant i \leqslant k} |\Delta u_i|, \quad \zeta'_k = \max_{1 \leqslant i \leqslant k} |\delta u_i|. \tag{24}$$

We denote by p_ξ the probability density function (PDF) of a random variable ξ, and by $p_{\zeta,k}$ the PDF p_{ζ_k}. We will first compare the PDF's $p_{\zeta,n'}$ as simulated by the Randomization method, a direct Monte Carlo simulation, and the Fourier-wavelet method.

The procedure of direct Monte Carlo simulation (DMS) of the collection of random variables Δu_i, $i = 1, \ldots, n'$, can be described as follows. These random variables are Gaussian with zero mean and covariance

$$\langle \Delta u_i \Delta u_j \rangle = \frac{1}{2J_\alpha h^{\alpha-1}} [D((i-j+1)h) + D((i-j-1)h) - 2D((i-j)h)].$$

Note that if $\rho k_0 \ll 1$, $D(\rho)$ can be replaced by $J_\alpha \rho^{\alpha-1}$. Therefore, if $n' h k_0 \ll 1$, the covariance can be approximated by

$$B_{ij} = \frac{1}{2}(|i-j+1|^{\alpha-1} + |i-j-1|^{\alpha-1} - 2|i-j|^{\alpha-1}), \quad i, j = 1, \ldots, n'. \tag{25}$$

Thus the DMS procedure is simply the direct simulation of Gaussian variables with covariance matrix given by (25). An analogous DMS procedure can be constructed for the random variables δu_i, $i = 1, \ldots, n'$. This DMS approach is of course impractical for actually simulating the values of a multiscale random field over a large number of points, as discussed in Section 5.1.1.

All numerical simulations in this section refer to the random field with Kolmogorov spectrum (15). In calculations of PDFs, we choose the parameters as follows: $h = 1000\ell_{\min}$, $\ell_{\min} = 2^{-40}$, $n' = 100$, and $q_0 = 1.115$. In Fig. 7, left panel, we show the PDF $p_{\zeta,100}$ calculated by the Randomization method with $n = 40$ sampling bins, bin ratio $q = 2$, and various values for the number of wavenumbers per sampling bin n_0. To analyze the accuracy in the PDF calculations, we plot in the right panel of Fig. 7 the corresponding deviations measured in L_2-norm and defined as follows: $\epsilon(k) = \|p_{\zeta,k}^{(\mathrm{DMS})} - \tilde{p}_{\zeta,k}\|_{L_2}$, where $p_{\zeta,k}^{(\mathrm{DMS})}$ is an approximation of the density

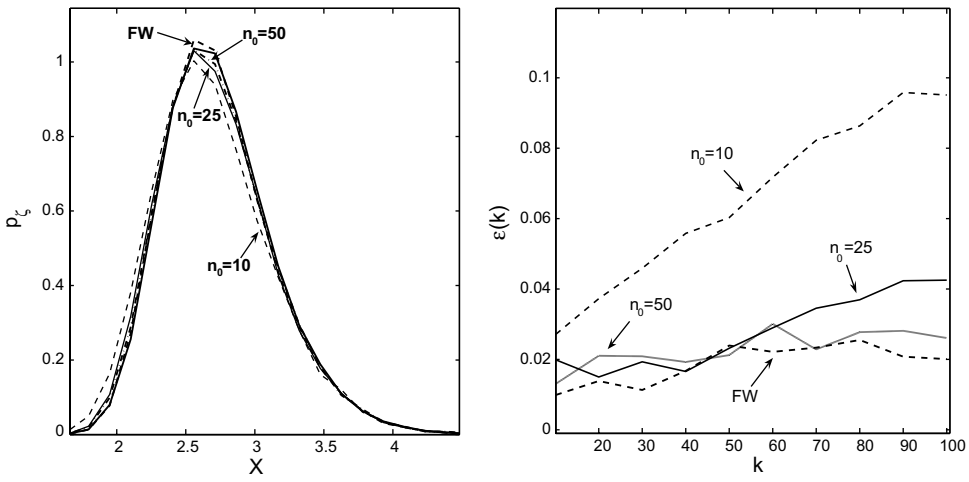

Fig. 7. Left panel: Probability density function $p_{\zeta,100}$ for $\zeta_{100} = \max_{1 \leqslant i \leqslant 100} |\Delta u_i|$ (23) calculated by the Randomization method with $n_0 = 10$ (thin dashed line), $n_0 = 25$ (thin solid line), and $n_0 = 50$ (bold dashed point line) wavenumbers per bin, by the Fourier-wavelet method (bold dashed line), and by the DMS method (bold solid line). Right panel: Deviation in L_2-norm between the PDFs calculated by the DMS and Randomization methods, for different values of n_0. For comparison the deviation is shown also between the DMS and Fourier-wavelet method.

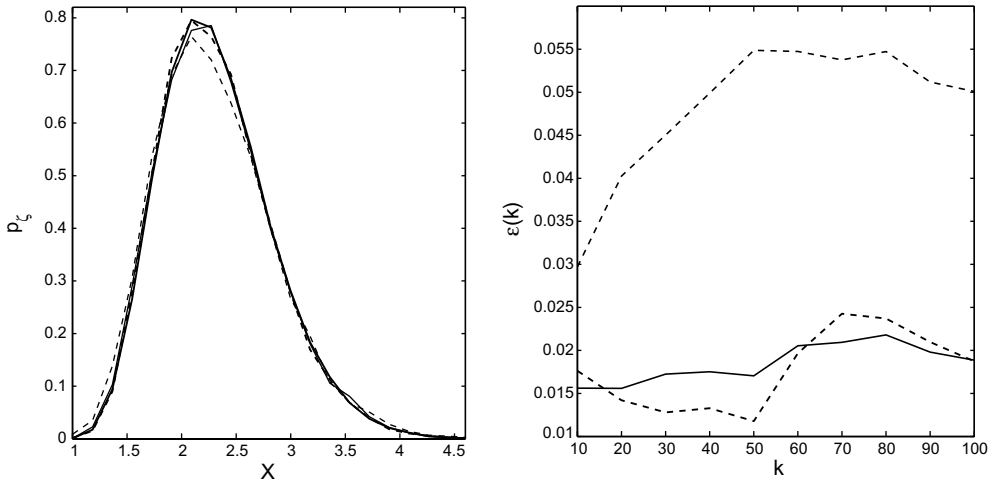

Fig. 8. Left panel: Probability density function $p_{\zeta',100}$ for $\zeta'_{100} = \max_{1\leqslant i\leqslant 100}|\delta u_i|$ (23) calculated by the Randomization method with $n_0 = 1$ (thin dashed line) and $n_0 = 4$ (thin solid line), by the Fourier-wavelet method (bold dashed line), and by the DMS method (bold solid line). Right panel: Deviation in L_2-norm between the PDFs calculated by the DMS and Randomization methods, for $n_0 = 1$ (thin dashed line), and $n_0 = 4$ (solid line). For comparison the deviation is shown also between DMS and Fourier-wavelet method (bold dashed line).

$p_{\zeta,k}$ obtained by direct Monte Carlo simulation with $N_s = 10^5$ samples (which we take as an accurate representation of the true PDF) and $\tilde{p}_{\zeta,k}$ denotes the corresponding approximation obtained by the Randomization or Fourier-wavelet methods with $N_s = 25{,}000$ samples. We see that the error of the Randomization method with $n_0 = 10$ wavenumbers per bin is large for all values of k. With $n_0 = 25$, this method has approximately the same accuracy as the Fourier-wavelet method for $k \leqslant 50$. Finally, calculations with $n_0 = 50$ show that the Randomization method gives over the whole displayed range of k almost the same quality as the Fourier-wavelet method. We remark that since the Fourier-wavelet method generates theoretically Gaussian multi-point statistics, its accuracy in simulating multi-point statistics of a Gaussian random field is completely determined by the number of Monte Carlo samples and its accuracy in simulating the correct second order correlation function.

One might conclude from Fig. 7 that in the case of multi-point statistical characteristics, the Randomization method is not competitive with the Fourier-wavelet method, as the number of wavenumbers per bin n_0 must be quite large for good accuracy. (The two methods have approximately equal cost if $n_0 = 10$.) However, if we consider the PDF and relevant deviations for the random variables ζ'_k (24) plotted in Fig. 8, we see that the Randomization method is competitive with the Fourier-wavelet method here since it achieves comparable accuracy already for $n_0 = 4$ wavenumbers per bin. So some multi-point statistics of Gaussian random fields are more efficiently simulated by the Fourier-wavelet method, but some can be captured with reasonable effort also by the Randomization method.

8. Conclusions

(1) The Randomization method is generally easier to implement than the Fourier-wavelet method. For simulating random fields with accurate two-point statistics, the Randomization method with logarithmically uniform spectral subdivision can often be less expensive than that of the Fourier-wavelet method. The scenario with greatest relative advantage for the Randomization method appears to be the sampling of a multiscale random field over a large but sparse set of points. Then, as is generally case, the cost of the Randomization method scales linearly with the number N_e of evaluation points and logarithmically in the range of scales $\ell_{\max}/\ell_{\min}$ to be represented in the random field. A relatively simple implementation of the Fourier-wavelet method (pre-computation of all random variables) has cost scaling linearly (and additively) in both the number of evaluations N_e and the ratio of the largest and smallest scales

of the random field simulated, $\ell_{\max}/\ell_{\min}$. A more sophisticated management of random numbers in the code can reduce the cost scaling of the Fourier-wavelet method in this scenario to the same as that of the Randomization method, but with a typically larger prefactor.

(2) The reason for the relative efficiency of the Randomization method in simulating two-point statistics accurately is that it appears adequate to use a fixed number $n_0 \sim 4$–10 of random variables to represent the random field at each length scale. The Fourier-wavelet method uses, as part of its essential design, $2^m(L/\ell_{\max})$ random variables to represent the random field structure over a computational domain of linear extent L at length scale $2^{-m}\ell_{\max}$. In particular, the Fourier-wavelet method uses many more random variables to represent the random field structure at smaller scales.

(3) Both the Randomization method and the simple implementation of the Fourier-wavelet method have comparable scaling when the random field is to be simulated over a regular computational grid of points, because the number of evaluations are comparable to the number of random variables in the Fourier-wavelet representation.

(4) The cost of the Randomization method increases substantially as statistics involving larger numbers of points are to be simulated accurately. The reason is that the number of computational elements (wavenumbers) per scale, n_0 must be increased to achieve accuracy with these more complex statistics. The Fourier-wavelet method, on the other hand, from the start employs a rich set of computational elements and random variables, and does not require a substantial increase in computational effort to simulate statistics involving large numbers of points accurately. This general conclusion does not however imply that the Randomization method will necessarily be less efficient than the Fourier-wavelet method for calculating every multi-point statistical characteristic, as our calculations in Fig. 8 show.

(5) When statistics are to be evaluated through spatial averages (and an appeal to ergodicity) rather than ensemble averages, the Fourier-wavelet method appears more efficient than the Randomization method. Good ergodic properties are important in applications which involve the solution of partial differential equations with random coefficients, such as the Darcy equation with random hydraulic conductivity.

Acknowledgments

This work is partly supported by Grants: German DFG Grant 436 TUK 17/1/05, Russian RFBR Grant N 06-01-00498, NATO Linkage Grant CLG 981426. P.R.K. is partly supported by an NSF grant DMS-0207242.

Appendix A. Calculation of the functions f_m

Here we give some technical details on the calculation of the functions (10) which in our case reads

$$f_m(\xi) = \int_{-4/3}^{4/3} \mathrm{e}^{-2\pi \mathrm{i} k\xi} g(k)\, \mathrm{d}k, \tag{A.1}$$

where $g(k) = 2^{m/2}\tilde{E}^{1/2}(2^m k)\hat{\phi}(k)$.

We calculate this function on the grid of points $\xi_j = -\frac{N}{2}\Delta\xi + (j-1)\Delta\xi$, $j = 1, \ldots, N$, where N is an even number, and $\Delta\xi \geqslant 0$ is the grid step. In order to evaluate the truncated sums appearing in the Fourier-wavelet representation (14), we must choose $N\Delta\xi/2 \geqslant b$. We approximate the integral (A.1) by a Riemann sum:

$$f_m(\xi_j) = \int_{-a}^{a} \mathrm{e}^{-2\pi \mathrm{i} k\xi} g(k)\, \mathrm{d}k \simeq \sum_{l=1}^{N} \Delta k \mathrm{e}^{-2\pi \mathrm{i} k_l \xi_j} g(k_l), \tag{A.2}$$

where

$$k_l = -a + (l - 1/2)\Delta k, \quad l = 1, \ldots, N; \quad \Delta k = \frac{2a}{N}.$$

We use the same number of points $N = 2^r$ (where r is some positive integer) to discretize the integral as we use to represent $f_m(\xi)$ in physical space so that we can use the discrete fast Fourier transform. We also clearly need

the cutoff on the integral in (A.2) to satisfy $a > 4/3$ (with $g(k)$ set to zero whenever evaluated for $|k| > 4/3$). Finally, the use of the fast Fourier transform requires the steps in physical and wavenumber space be related through $\Delta\xi\Delta k = 1/N$. Indeed, simple transformations then yield

$$\begin{aligned}\xi_j k_l &= \left[-\frac{N}{2}\Delta\xi + (j-1)\Delta\xi\right][-a + (l-1/2)\Delta k] \\ &= \frac{N-1}{4} - \frac{j-1}{2}\left(1-\frac{1}{N}\right) - \frac{l-1}{2} + \frac{(j-1)(l-1)}{N},\end{aligned} \tag{A.3}$$

hence

$$f_m(\xi_j) \simeq \exp\left\{\pi\mathrm{i}(j-1)\left(1-\frac{1}{N}\right)\right\}\sum_{l=1}^{N} G_l \exp\left\{-2\pi\mathrm{i}\frac{(j-1)(l-1)}{N}\right\}, \tag{A.4}$$

where

$$G_l = \Delta k g(k_l)\exp\left\{-2\pi\mathrm{i}\left[\frac{N-1}{4} - \frac{l-1}{2}\right]\right\},$$

which is in the form of a discrete Fourier transform.

The constraints imposed on the discretization of the integral (A.2) to obtain an expression amenable to fast Fourier transform imply the following sequence of choosing parameters. First a bandwidth value b is chosen according to the desired accuracy in the Fourier-wavelet representation (14). Then a spatial resolution $\Delta\xi$ for the $f_m(\xi)$ is selected, either according to the grid spacing h on a prespecified set of evaluation points or such that $f_m(\xi)$ can be calculated accurately enough by interpolation from the computed values. (In any event, we must have $\Delta\xi < 3/8$). Next, a binary power $N = 2^r$ is chosen large enough so that $2b/N \leqslant \Delta\xi$. Then we set $a = \frac{1}{2\Delta\xi}$, and discretize the integral (A.2) with step size $\Delta k = 2a/N = 1/(N\Delta\xi)$.

References

[1] N.A. Buglanova, O. Kurbanmuradov, Convergence of the randomized spectral models of homogeneous Gaussian random fields, Monte Carlo Methods Appl. 1 (3) (1995) 173–201.
[2] Chris Cameron, Relative efficiency of Gaussian stochastic process sampling procedures, J. Comput. Phys. 192 (2) (2003) 546–569.
[3] René A. Carmona, Stanislav A. Grishin, Stanislav A. Molchanov, Massively parallel simulations of motions in a Gaussian velocity field, in: Stochastic Modelling in Physical Oceanography, Progr. Prob., vol. 39, Birkhäuser, Boston, 1996, pp. 47–68.
[4] D. Cioranescu, P. Donato, An Introduction to Homogenization, Oxford University Press, New York, 1999.
[5] G. Dagan, A. Fiori, I. Janković, Flow and transport in highly heterogeneous formations: 1. Conceptual framework and validity of first-order approximations, Water Resour. Res. 39 (9) (2003) 1268.
[6] Frank W. Elliott Jr., David J. Horntrop, Andrew J. Majda, A Fourier-wavelet Monte Carlo method for fractal random fields, J. Comput. Phys. 132 (2) (1997) 384–408.
[7] Frank W. Elliott Jr., David J. Horntrop, Andrew J. Majda, Monte Carlo methods for turbulent tracers with long range and fractal random velocity fields, Chaos 7 (1) (1997) 39–48.
[8] Frank W. Elliott Jr., Andrew J. Majda, A wavelet Monte Carlo method for turbulent diffusion with many spatial scales, J. Comput. Phys. 113 (1) (1994) 82–111.
[9] Frank W. Elliott Jr., Andrew J. Majda, A new algorithm with plane waves and wavelets for random velocity fields with many spatial scales, J. Comput. Phys. 117 (1995) 146–162.
[10] Frank W. Elliott Jr., Andrew J. Majda, Pair dispersion over an inertial range spanning many decades, Phys. Fluids 8 (4) (1996) 1052–1060.
[11] A. ElMaihy, F. Nicolleau, Investigation of the dispersion of heavy-particle pairs and Richardson's law using kinematic simulation, Phys. Rev. E 71 (4) (2005) 046307.
[12] Jens Feder, Fractals, Physics of Solids and Liquids, Plenum Press, New York and London, 1988, pp. 163–243 (Chapters 9–14).
[13] William Feller, An Introduction to Probability Theory and its Applications, second ed., vol. 2, Wiley, New York, London, 1971, pp. 47, 48 (Section III.6).
[14] Uriel Frisch, Turbulence, Cambridge University Press, Cambridge, 1995, The legacy of A.N. Kolmogorov.
[15] J.C.H. Fung, J.C.R. Hunt, N.A. Malik, R.J. Perkins, Kinematic simulation of homogenous turbulence by unsteady random Fourier modes, J. Fluid Mech. 236 (1992) 281–318.
[16] J.C.H. Fung, J.C. Vassilicos, Two-particle dispersion in turbulent like flows, Phys. Rev. E (3) 57 (2, part A) (1998) 1677–1690.
[17] I.M. Gel'fand, G.E. Shilov, Generalized Functions. Properties and Operations, vol. 1, Academic Press, New York, 1964 (Section 3.3).
[18] Lynn W. Gelhar, Stochastic Subsurface Hydrology, Prentice-Hall, Englewood Cliffs, NJ, 1993.

[19] D. Horntrop, A. Majda, An overview of Monte Carlo simulation techniques for the generation of random fields, in: P. Muller, D. Henderson (Eds.), Monte Carlo Simulations in Oceanography, Proceedings of the Ninth 'Aha Huliko'a Hawaiian Winter Workshop, 1997, pp. 67–79.
[20] M.A.I. Khan, A. Pumir, J.C. Vassilicos, Kinematic simulation of turbulent dispersion of triangles, Phys. Rev. E 68 (2) (2003) 026313.
[21] Peter E. Kloeden, Eckhard Platen, Numerical Solution of Stochastic Differential Equations, Applications of Mathematics: Stochastic Modelling and Applied Probability, vol. 23, Springer, Berlin, 1992.
[22] Dmitry Kolyukhin, Karl Sabelfeld, Stochastic flow simulation in 3D porous media, Monte Carlo Methods Appl. 11 (1) (2005) 15–37.
[23] R.H. Kraichnan, Diffusion by a random velocity field, Phys. Fluids 13 (1) (1970) 22–31.
[24] O. Kurbanmuradov, Weak convergens of approximate models of random fields, Russ. J. Numer. Anal. Math. Modelling 10 (6) (1995) 500–517.
[25] O. Kurbanmuradov, Weak convergence of randomized spectral models of Gaussian random vector fields, Bull. Novosibirsk Computing Center, Numer. Anal. (4) (1993) 19–25.
[26] O. Kurbanmuradov, K. Sabelfeld, D. Koluhin, Stochastic Lagrangian models for two-particle motion in turbulent flows, Numer. Results, Monte Carlo Methods Appl. 3 (3) (1997) 199–223.
[27] N.N. Lebedev, Special Functions and their Applications, Dover, New York, 1972, pp. 1–15 (Chapter 1).
[28] Marcel Lesieur, Turbulence in Fluids, second revised ed., Number 1 in Fluid Mechanics and its Applications, Kluwer, Dordrecht, 1990.
[29] Andrew J. Majda, Peter R. Kramer, Simplified models for turbulent diffusion: theory, numerical modelling, and physical phenomena, Phys. Rep. 314 (4-5) (1999) 237–574.
[30] Stéphane Mallat, A Wavelet Tour of Signal Processing, Academic Press, San Diego, CA, 1998.
[31] Benoit B. Mandelbrot, The Fractal Geometry of Nature, Updated and Augmented Edition, Freeman, San Francisco, New York, 1983.
[32] W.D. McComb, The Physics of Fluid Turbulence, Oxford Engineering Science Series, vol. 25, Clarendon Press, New York, 1991 (Chapter 2).
[33] G.A. Mikhailov, Approximate models of random processes and fields, Russ. J. Comp. Math. Math. Phys. 23 (3) (1983) 558–566 (in Russian).
[34] A.S. Monin, A.M. Yaglom, Statistical Fluid Mechanics: Mechanics of Turbulence, vol. 2, MIT Press, 1981.
[35] F. Poirion, C. Soize, Numerical methods and mathematical aspects for simulation of homogenous and non homogenous Gaussian vector fields, in: Paul Kree, Walter Wedig (Eds.), Probabilistic Methods in Applied Physics, Lecture Notes in Physics, vol. 451, Springer, Berlin, 1995, pp. 17–53.
[36] Stephen B. Pope, Turbulent Flows, Cambridge University Press, Cambridge, 2000.
[37] William H. Press, Saul A. Teukolsky, William T. Vetterling, Brian P. Flannery, Numerical Recipes in FORTRAN, second ed., Cambridge University Press, Cambridge, 1992, Section 7.8, pages xxvi + 963, The art of scientific computing, With a separately available computer disk..
[38] Bénédicte Puig, Fabrice Poirion, White noise and simulation of ordinary Gaussian processes, Monte Carlo Methods Appl. 10 (1) (2004) 69–89.
[39] Yoram Rubin, Applied Stochastic Hydrogeology, Oxford University Press, New York, 2003.
[40] K.K. Sabelfeld, O. Kurbanmuradov, Stochastic Lagrangian models for two-particle motion in turbulent flows, Monte Carlo Methods Appl. 3 (1) (1997) 53–72.
[41] K.K. Sabelfeld, O. Kurbanmuradov, Two-particle stochastic Eulerian–Lagrangian models of turbulent dispersion, Math. Comput. Simul. 47 (2–5) (1998) 429–440, IMACS Seminar on Monte Carlo Methods (Brussels, 1997).
[42] Karl K. Sabelfeld, Monte Carlo Methods in Boundary Value Problems, Springer Series in Computational Physics, Springer, Berlin, 1991, Chapters 1, 5, pp. 31–47, 228–238.
[43] M. Shinozuka, Simulation of multivariate and multidimensional random processes, J. Acoust. Soc. Am. 49 (1971) 357–368.
[44] H. Sigurgeirsson, A.M. Stuart, A model for preferential concentration, Phys. Fluids 14 (12) (2002) 4352–4361.
[45] D.J. Thomson, B.J. Devenish, Particle pair in kinematic simulations, J. Fluid Mech. 526 (2005) 277–302.
[46] J.A. Viecelli, E.H. Canfield Jr., Functional representation of power-law random fields and time series, J. Comput. Phys. 95 (1991) 29–39.
[47] Richard F. Voss, Random fractal forgeries, in: Rae A. Earnshaw (Ed.), Fundamental Algorithms for Computer Graphics, NATO ASI Series F: Computer and System Sciences, vol. 17, Springer, Berlin, 1985, pp. 805–835 (NATO Science Affairs Division).
[48] A.M. Yaglom, Correlation Theory of Stationary and Related Random Functions, Basic Results, vol. I, Springer, Berlin, 1987.